AMERICAN SOCIETY FOR MICROBIOLOGY | Antimicrobial Agents and Chemotherapy®

MECHANISMS OF RESISTANCE

The Set1 Histone H3K4 Methyltransferase Contributes to Azole Susceptibility in a Species-Specific Manner by Differentially Altering the Expression of Drug Efflux Pumps and the Ergosterol Gene Pathway

Kortany M. Baker,[a] Smriti Hoda,[a] Debasmita Saha,[a] Justin B. Gregor,[a] Livia Georgescu,[a] Nina D. Serratore,[a]* Yueping Zhang,[a§] Lizhi Cheng,[a] Nadia A. Lanman,[b,c] Scott D. Briggs[a,b]

[a]Department of Biochemistry, Purdue University, West Lafayette, Indiana, USA
[b]Purdue University Center for Cancer Research, Purdue University, West Lafayette, Indiana, USA
[c]Department of Comparative Pathobiology, Purdue University, West Lafayette, Indiana, USA

ABSTRACT Fungal infections are a major health concern because of limited antifungal drugs and development of drug resistance. *Candida* can develop azole drug resistance by overexpression of drug efflux pumps or mutating *ERG11*, the target of azoles. However, the role of epigenetic histone modifications in azole-induced gene expression and drug resistance is poorly understood in *Candida glabrata*. In this study, we show that Set1 mediates histone H3K4 methylation in *C. glabrata*. In addition, loss of *SET1* and histone H3K4 methylation increases azole susceptibility in both *C. glabrata* and *S. cerevisiae*. This increase in azole susceptibility in *S. cerevisiae* and *C. glabrata* strains lacking *SET1* is due to distinct mechanisms. For *S. cerevisiae*, loss of *SET1* decreased the expression and function of the efflux pump Pdr5, but not *ERG11* expression under azole treatment. In contrast, loss of *SET1* in *C. glabrata* does not alter expression or function of efflux pumps. However, RNA sequencing revealed that *C. glabrata* Set1 is necessary for azole-induced expression of all 12 genes in the late ergosterol biosynthesis pathway, including *ERG11* and *ERG3*. Furthermore, chromatin immunoprecipitation analysis shows histone H3K4 trimethylation increases upon azole-induced *ERG* gene expression. In addition, high performance liquid chromatography analysis indicated Set1 is necessary for maintaining proper ergosterol levels under azole treatment. Clinical isolates lacking *SET1* were also hypersusceptible to azoles which is attributed to reduced *ERG11* expression but not defects in drug efflux. Overall, Set1 contributes to azole susceptibility in a species-specific manner by altering the expression and consequently disrupting pathways known for mediating drug resistance.

KEYWORDS azole, *Candida glabrata*, *ERG11*, epigenetics, H3K4 methylation, Set1, antifungal resistance, ergosterol, histone methylation, regulation of gene expression

Candida infections are a major health concern due to the increased frequency of infections and the development of drug resistance (1, 2). Over the years, *Candida glabrata* has become the second most common cause of candidiasis (1–3). In some immunocompromised patients, such as diabetics, patients with hematologic cancer, organ transplant recipients, and the elderly, it is the most predominant *Candida* infection (2–6). The emergence of *C. glabrata* as a major pathogen is likely due to its intrinsic drug resistance to azole antifungal drugs and ability to quickly adapt and acquire clinical drug resistance during treatment (3, 7). The consequence of drug resistance leads to increases in health care costs, as well as lower success rates in treatment and an increase in mortality (8–10).

C. glabrata naturally has low susceptibility to azole drugs and consequently, echinocandins are the preferred drug choice for treating *C. glabrata* infections (11). *C. glabrata* can also acquire clinical resistance to azole drugs which is often due to overexpressing the ABC-transporter

Address correspondence to Scott D. Briggs, sdbriggs@purdue.edu.

*Present address: Nina D. Serratore, Cook Research Incorporated, West Lafayette, Indiana, USA.

§Present address: Yueping Zhang, College of Veterinary Medicine, China Agricultural University, Beijing, China.

The authors declare no conflict of interest.

Received 24 November 2021
Returned for modification 12 December 2021
Accepted 10 April 2022
Published 26 April 2022

drug efflux pump Cdr1 or Pdh1 (Cdr2) caused by gain-of-function mutations in the transcription factor Pdr1 (7, 12–14). In other *Candida* species, acquired clinical azole resistance can also be due to overexpression of *ERG11* due to gain-of-function mutations in the Upc2 transcription factor or mutations in *ERG11* (15–17). However, for unknown reasons, *ERG11* or *UPC2* mutations are typically not found in clinically drug-resistant *C. glabrata* strains (7, 18–20).

Because pathogenic fungi can rapidly adapt to various cellular environments and xenobiotic drug exposures, epigenetic mechanisms are also likely contributing to altered gene expression profiles permissive for adaptation and drug resistance. Several studies in *Candida albicans* support this hypothesis and show that epigenetic factors such as histone acetyltransferases, *Ca*Gcn5 and *Ca*Rtt109, and histone deacetylases, *Ca*Rpd3 and *Ca*Hda1 are important for either fungal pathogenesis and/or drug resistance (21–25). In contrast, epigenetic factors that posttranslationally modify histones have not been extensively studied for their roles in drug resistance in *C. glabrata*. Nonetheless, Orta-Zavalz et al. have shown that deleting histone deacetylase, *CgHST1*, decreases susceptibility to fluconazole, which is likely attributed to an increase in transcript levels of *CgPDR1* and *CgCDR1* under untreated conditions (26). In addition, a recent publication by Filler et al., has indicated that *C. glabrata* strains with *CgGCN5*, *CgRPD3*, or *CgSPP1* deleted have increased susceptibility to caspofungin when using high concentrations (27). However, no mechanistic understanding such as gene targets or changes in chromatin/histone modifications was provided for the caspofungin-hypersensitive phenotype.

Previous publications from our lab demonstrated that in *Saccharomyces cerevisiae* loss of Set1, a known histone H3K4 methyltransferase, has a hypersensitive growth defect in the presence of the antifungal metabolite, brefeldin A (BFA) and clinically used azole drugs (28, 29). We determined that hypersensitivity to BFA was due to a decrease in ergosterol levels in *S. cerevisiae* strains lacking histone H3K4 methylation. However, until this study, no mechanistic understanding has been provided why *S. cerevisiae* or *C. glabrata* strains lacking *SET1* alter azole drug susceptibility. Furthermore, in *C. albicans*, loss of *SET1* appears to alter virulence but not azole drug resistance (30). To determine whether an increase in azole susceptibility is conserved in a human fungal pathogen that is evolutionarily closer to *S. cerevisiae* than *C. albicans*, we investigated the role of Set1 and its mechanistic contribution to altering azole susceptibility in *S. cerevisiae* and *C. glabrata*.

Here, we show for the first time that Set1-mediates histone H3K4 mono-, di-, and trimethylation in *C. glabrata* and loss of Set1-mediated histone H3K4 methylation alters the azole drug susceptibility of *C. glabrata* similar to what is seen in *S. cerevisiae*. Interestingly, azole hypersusceptibility in *S. cerevisiae* lacking *SET1* appears to be mediated by a decrease in the expression and function of *Sc*Pdr5, the *Cg*Cdr1 ortholog, and not a failure to induce *ERG* genes. However, hypersusceptibility to azole drugs in *C. glabrata* strains lacking Set1-mediated histone H3K4 methylation is not a consequence of altered expression levels of *CgCDR1*, *CgPDR1* or their ability to efflux drugs. Interestingly, RNA sequencing (RNA-seq) and HPLC analysis revealed that *Cg*Set1 is required for azole-induced expression of *CgERG* genes, including *CgERG11* and *CgERG3*, so that proper ergosterol levels are maintained. Azole-induced gene expression was dependent on Set1 methyltransferase activity and associated with gene-specific increases in histone H3K4 trimethylation on *CgERG11* and *CgERG3* chromatin. In addition, clinical isolates lacking *CgSET1* were hypersensitive to azoles and attributed to reduced *CgERG11* expression but not reduced efflux pump function. Overall, we show that loss of Set1-mediated histone H3K4 methylation in *S. cerevisiae* and *C. glabrata* contributes to azole hypersusceptibility by distinct mechanisms where genes, known for drug resistance, are differentially altered. Identifying and understanding the epigenetic mechanisms contributing to altered drug efficacy in various fungal species will be important for the development of alternative drug targets for treating patients with fungal infections.

RESULTS

Loss of Set1-mediated histone H3K4 methylation in *S. cerevisiae* and *C. glabrata* increases azole drug susceptibility. Set1 is a known SET domain-containing lysine histone methyltransferase that is conserved from yeast to humans and the enzymatic activity of the SET domain catalyzes mono-, di-, and trimethylation on histone H3 at lysine 4 (Lys4) (31, 32).

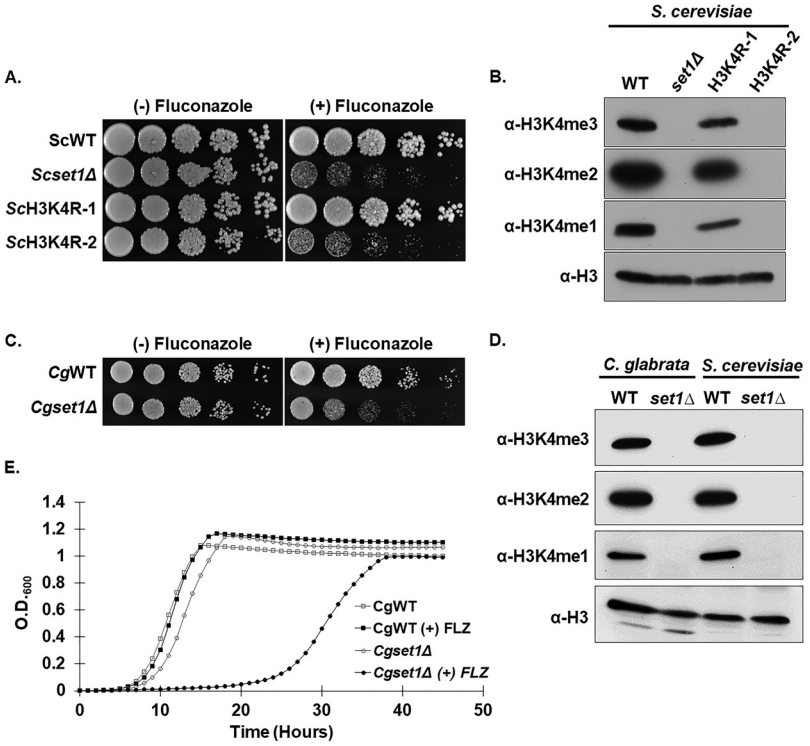

FIG 1 Loss of Set1-mediated mono-, di-, and trimethylation at histone H3K4 in *S. cerevisiae* and *C. glabrata* results in increased azole susceptibility and delayed growth *in vitro*. (A) Fivefold serial dilution spot assays of the indicated *S. cerevisiae* strains were grown on SC media with and without 8 μg/mL fluconazole and incubated at 30°C for 72 h. (B and D) Whole-cell extracts isolated from the indicated strains were immunoblotted using histone H3K4 methyl-specific mono-, di-, and trimethylation antibodies of whole-cell extracts isolated from the indicated strains. Histone H3 was used as a loading control. (C) Fivefold serial dilution spot assays of the indicated *C. glabrata* strains were grown on SC media with or without 32 μg/mL fluconazole and incubated at 30°C for 48 h. (E) Liquid growth curve assay of the indicated *C. glabrata* strains grown over 50 h with or without 32 μg/mL fluconazole.

Our previous work in *S. cerevisiae* has determined that loss of *SET1* in the BY4741 background strain results in increased susceptibility to azole drugs, suggesting that H3K4 methylation is necessary for mediating wild-type azole drug resistance (29). To determine the role of histone H3K4 methylation in azole drug efficacy, we constructed histone H3K4R mutations in the BY4741 background strain. Because *S. cerevisiae* has two genes encoding histone H3, two yeast strains were constructed where a histone H3K4R mutation was integrated at one histone H3 gene keeping the other gene wild type (*Sc*H3K4R-1), while the other strain contained H3K4R mutations integrated at both histone H3 genes (*Sc*H3K4R-2; see Table S1 in the supplemental material). To determine whether a loss of histone H3K4 methylation altered azole drug sensitivity similar to a *set1*Δ (*Scset1*Δ) strain, a serial-dilution spot assay was performed. Both *Scset1*Δ and *Sc*H3K4R mutant strains were grown in SC complete media and spotted onto SC agar plates with or without 8 μg/mL fluconazole (Fig. 1A). These data show that loss of histone H3K4 methylation by deleting *ScSET1* or mutating histone H3 where both histone H3 genes are mutated at K4 (*Sc*H3K4R-2), resulted in similar azole drug hypersensitivity compared to each other (Fig. 1A). To confirm that histone H3K4 methylation was abolished in these strains, Western blot analysis was performed using methyl-specific antibodies to detect histone H3K4 mono-, di-, and trimethylation (Fig. 1B). Histone H3 was used for a loading control (Fig. 1B). As expected, histone methylation was abolished in *set1*Δ and in H3K4R-2 mutation strains but not in the histone H3K4R-1 strain (Fig. 1B). Together, our data demonstrate that the presence of histone H3K4 methylation is critical for maintaining wild-type azole drug susceptibility.

To determine whether an azole hypersensitive growth phenotype observed in *S. cerevisiae* is also conserved in the human fungal pathogen *C. glabrata*, the WT (*Cg*WT) and a *set1*Δ (*Cgset1*Δ) strain were spotted on SC agar plates with and without

A.

Strain (CBS138)	FLZ (μg/mL) in RPMI
*Cg*WT	64
Cgset1Δ	8
Cgswd1Δ	8
Cgspp1Δ	16
Cgbre2Δ	16

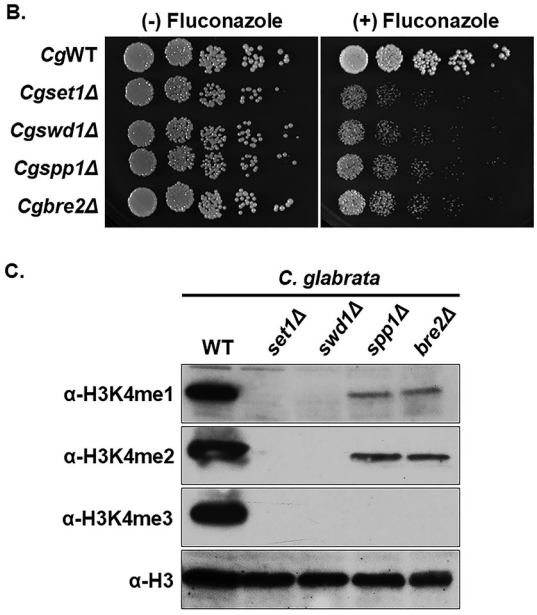

FIG 2 Deletion of Set1 complex members in *C. glabrata* results in increased azole susceptibility and loss of histone H3K4 methylation. (A) MIC assay of the indicated strains performed in RPMI 1640 media at 35°C, and results recorded after 48 h of incubation. (B) Fivefold serial dilution spot assays of the indicated *C. glabrata* strains were grown on SC plates with or without 32 μg/mL fluconazole. (C) Whole-cell extracts isolated from the indicated strains were immunoblotted using H3K4 methyl-specific mono-, di-, and trimethylation antibodies. Histone H3 was used as a loading control.

16 μg/mL fluconazole (Fig. 1C). Similar to what was observed in *S. cerevisiae*, deleting *SET1* in *C. glabrata* 2001 (CBS138, ATCC 2001) showed an increase in azole susceptibility compared to a *Cg*WT strain (Fig. 1C). In addition, the *Cgset1*Δ strain had a significant growth delay in liquid growth cultures compared to *Cg*WT when treated with 32 μg/mL fluconazole (Fig. 1E). Western blot analysis showed that deleting *CgSET1* abolished all histone H3K4 mono-, di-, and trimethylation confirming that *CgSET*1 is the sole histone H3K4 methyltransferase in *C. glabrata* (Fig. 1D). Altogether, our results show Set1-mediated histone H3K4 methylation in *S. cerevisiae* and *C. glabrata* is conserved and is necessary for maintaining a wild-type susceptibility to azole drugs.

Loss of *C. glabrata* Set1 complex members alters azole efficacy and histone H3K4 methylation. In *S. cerevisiae*, Set1 forms a complex referred to as the Complex Proteins Associated with Set1 or COMPASS. COMPASS forms a stable complex with eight proteins which includes the catalytic subunit Set1, Swd1, Swd2, Swd3, Spp1, Bre2, Sdc1, and Shg1 (33–35). Previous studies in *S. cerevisiae* have determined that Swd1, Swd2, Swd3, Spp1, Bre2, and Sdc1 are necessary for Set1 to properly catalyze the various states of histone H3K4 mono-, di-, and trimethylation (33–38). To determine whether COMPASS components are required for azole drug efficacy and Set1-mediated histone H3K4 methylation in *C. glabrata*, deletion strains lacking *SET1*, *SPP1*, *BRE2*, and *SWD1* were generated, and the MIC (in RPMI media) of each strain was determined (Fig. 2A). Consistent with *S. cerevisiae* serial-dilution spot and liquid growth assays in Fig. 1, the *Cgset1*Δ strain showed increased susceptibility to fluconazole with an 8-fold difference in MIC compared to the *Cg*WT strain (Fig. 2A).

A *Cgswd1*Δ strain showed a MIC similar to that of the *Cgset1*Δ strain, while the MICs of *Cgspp1*Δ and *Cgbre2*Δ deletion strains were 4-fold different than the WT strain (Fig. 2A). All *C. glabrata* COMPASS deletions strains showed an increase in susceptibility to azole drugs on agar plates similar to *S. cerevisiae* COMPASS deletion strains except for the *Scspp1*Δ strain, which is likely due to differences in the histone H3K4 methylation status (Fig. 2B and C; see also Fig. S1A) (29, 33, 34, 36, 38).

Western blot analysis determined that *Cgswd1*Δ strain lacked all forms of histone H3K4 methylation (Fig. 2C) which is also observed in *Cgset1*Δ and *Scset1*Δ strains (Fig. 2C and 1D). In contrast, deletion of *CgSPP1* and *CgBRE2* abolished all detectable levels of H3K4 trimethylation and significantly reduced the levels of histone H3K4 mono- and dimethylation. Taken together, our data show that when *C. glabrata* COMPASS subunits *SET1* and *SWD1* are deleted, global loss of histone H3K4 methylation is observed similar to what is seen when the subunits are deleted in *S. cerevisiae* (Fig. 2C) (33, 34, 36, 38). However, the *Cgspp1*Δ has a total loss of histone H3K4 trimethylation and significant loss of histone H3K4 mono- and dimethylation similar to the *Cgbre2*Δ and *Scbre2*Δ strains (Fig. 2C). For unknown reasons, the pattern of histone H3K4 methylation is different in the *Scspp1*Δ strain, which only has a reduction in histone H3K4 trimethylation but not mono- or dimethylation (33–39). Altogether, these results suggest that the COMPASS complex is needed to mediate proper histone H3K4 methylation and wild-type resistance to azole drugs.

Histone H3K4 methyltransferase activity of *C. glabrata* Set1 is necessary for wild-type growth on azole-containing media. To confirm that altered azole efficacy in the *Cgset1*Δ strain was due to loss of *SET1* and not a secondary mutation, a genomic fragment containing the *CgSET1* promoter, 5′ untranslated region (UTR), open reading frame, and the 3′ UTR was amplified by PCR and cloned into the *C. glabrata* plasmid, pGRB2.0 (40). Because a H1017K mutation in the SET domain of *S. cerevisiae* Set1 is known to be catalytically inactive (28, 41, 42), we performed site-directed mutagenesis on pGRB2.0-*CgSET1* and generated an analogous mutation in *C. glabrata* Set1 at H1048K determined using the sequence alignment in Fig. 3A. In addition, *SET1* was deleted in *C. glabrata* 2001HTU (ATCC 200989) to utilize the *ura3* auxotrophic marker (43). Importantly, *Cg*2001HTU lacking *SET1* was hypersensitive to azole drugs similar to when *SET1* was deleted in *Cg*2001 (Fig. 1C and Fig. 3B).

Furthermore, transformation of pGRB2.0-*CgSET1* into the *Cg*2001HTU/*set1*Δ strain was able to rescue azole hypersensitivity, while pGRB2.0-*Cgset1H1048K* did not rescue wild-type azole drug resistance, as shown by serial-dilution spot assays grown on SC agar plates with 32 μg/mL fluconazole (Fig. 3B). MIC assays under SC-ura conditions also show similar results (see Fig. S1B). Western blot analysis indicated that pGRB2.0-*CgSET1* expression in *Cg*2001HTU/*set1*Δ strain restored histone H3K4 methylation to wild-type levels, while *Cgset1H1048K* did not rescue histone H3K4 methylation confirming that this mutation lacks catalytic activity similar to *Scset1H1017K* (Fig. 3C). Importantly, quantitative real-time PCR analysis (qRT-PCR) confirmed that the plasmids expressing *CgSET1* and *Cgset1H1048K* were similar to the endogenously expressed *SET1* (see Fig. S1C). To ensure Set1 protein is expressed, a 3×FLAG sequence was inserted between the endogenous promoter and ATG of pGRB2.0-*cgSET1* WT and catalytically inactive plasmid. As expected, the strain expressing the 3×FLAG-*Cgset1H1048K* did not rescue H3K4 trimethylation and is hypersusceptible to fluconazole compared to a strain expressing 3×FLAG-*CgSET1*. Importantly, both wild-type and mutant *SET1* constructs are expressed at a similar protein level (see Fig. S1D and E). This shows that loss of histone H3K4 methylation was not due to difference in expression levels but due to the catalytic inactivation of *Cgset1H1048K*. These data suggest that azole hypersusceptibility in *Cgset1*Δ strains are specifically due to the loss of *SET1* and its catalytic activity.

Expression of drug efflux pumps are altered in a *S. cerevisiae set1*Δ strain but not in a *C. glabrata set1*Δ strain. In *Candida glabrata*, the major mechanisms for changes in drug resistance are due to altered expression of *CgCDR1*, the main drug efflux pump, or gain-of-function mutations in *CgPDR1*, a gene that encodes the transcription factor for *CgCDR1* (7, 12, 19, 20, 44). To determine whether altered drug resistance for *Scset1*Δ or *Cgset1*Δ strains are due to altered expression levels of the ATP-binding cassette (ABC) transporters *ScPDR5* or *CgCDR1*, respectively, the transcript levels of *ScPDR5* and *CgCDR1* were analyzed by qRT-PCR (Fig. 4). *Scset1*Δ cells grown with or without

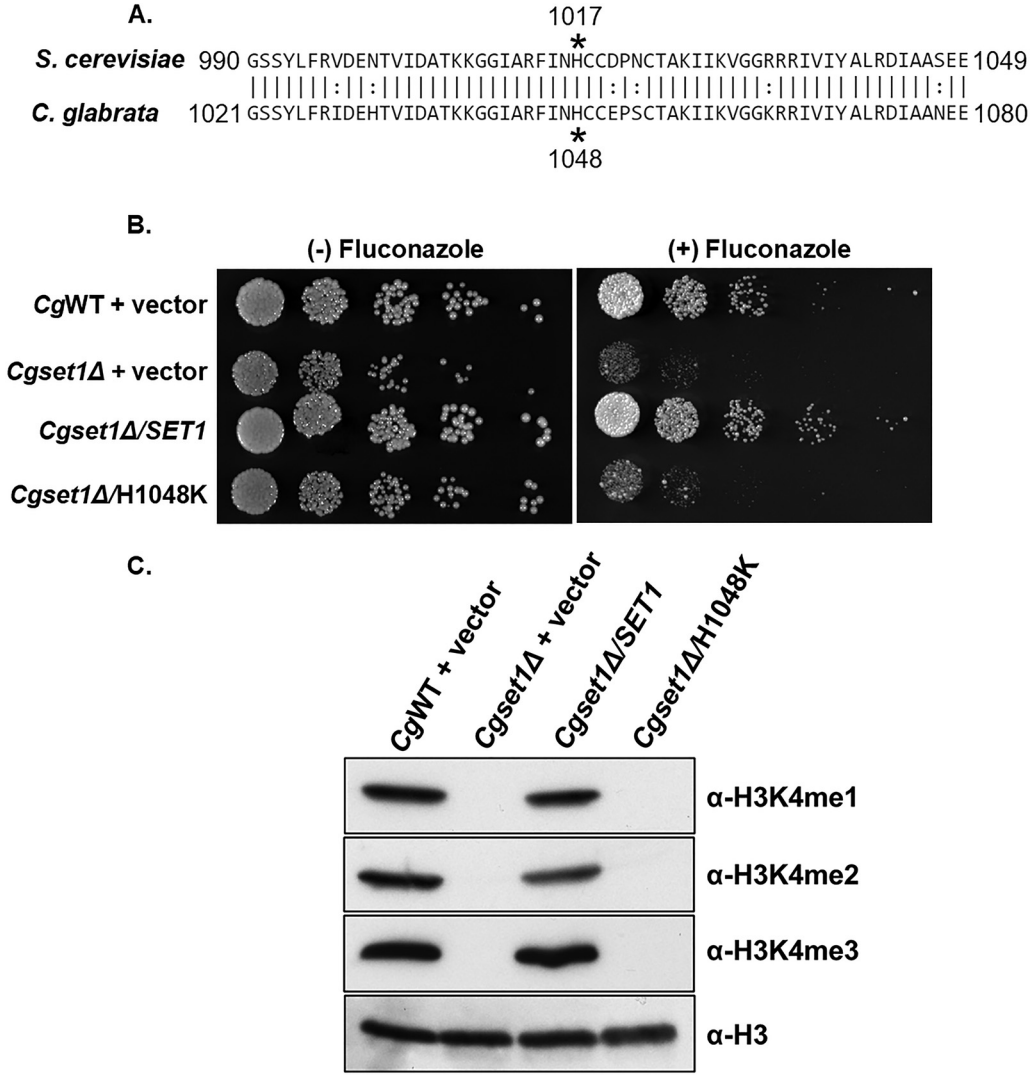

FIG 3 The catalytic activity of the SET domain is necessary for Set1-mediated histone H3K4 methylation and alters azole susceptibility in *C. glabrata*. (A) Sequence alignment comparing the SET domain amino acid residues of *S. cerevisiae* and *C. glabrata* Set1. Asterisks indicate residues required for catalytic activity. (B) Fivefold serial dilution spot assays of the indicated *C. glabrata* strains were grown on SC plates with or without 32 μg/mL fluconazole. (C) Whole-cell extracts isolated from the indicated strains were immunoblotted using methyl-specific mono-, di-, and trimethylation antibodies. Histone H3 was used as a loading control.

azoles showed a significant decrease in *ScPDR5* expression compared to WT cells (Fig. 4A). In addition, *Scset1*Δ cells did not have changes in *ScPDR1* transcripts, a gene encoding the transcription factor for *PDR5* (Fig. 4B). To determine whether drug efflux was reduced in *Scset1*Δ cells, a Nile red fluorescence-based assay was performed. Nile red, a fluorescent lipophilic stain, has been shown to be a substrate for the ABC-transporters and used as a proxy for drug efflux (45, 46). If Nile red is the substrate of an efflux pump (e.g., Pdr5), then cells expressing a functional efflux pump will not accumulate the dye and have low fluorescence. To show azole drugs induced efflux in *S. cerevisiae*, a Nile red fluorescence-based assay was performed on azole treated and untreated *Sc*WT cells. As expected, azole treated *Sc*WT cells had less fluorescence indicating an increase in Nile red efflux compared to *Sc*WT untreated cells (see Fig. S2D). Consistent with decreased expression of *PDR5* in *Scset1*Δ, azole-treated *Scset1*Δ cells had higher fluorescence than azole-treated *Sc*WT cells, indicating reduced efflux (Fig. 4C). A *Scpdr5*Δ strain was used as a positive control to prevent drug efflux (Fig. 4C).

In contrast, *CgCDR1* or *CgPDR1* expression was not altered in the *Cgset1*Δ cells

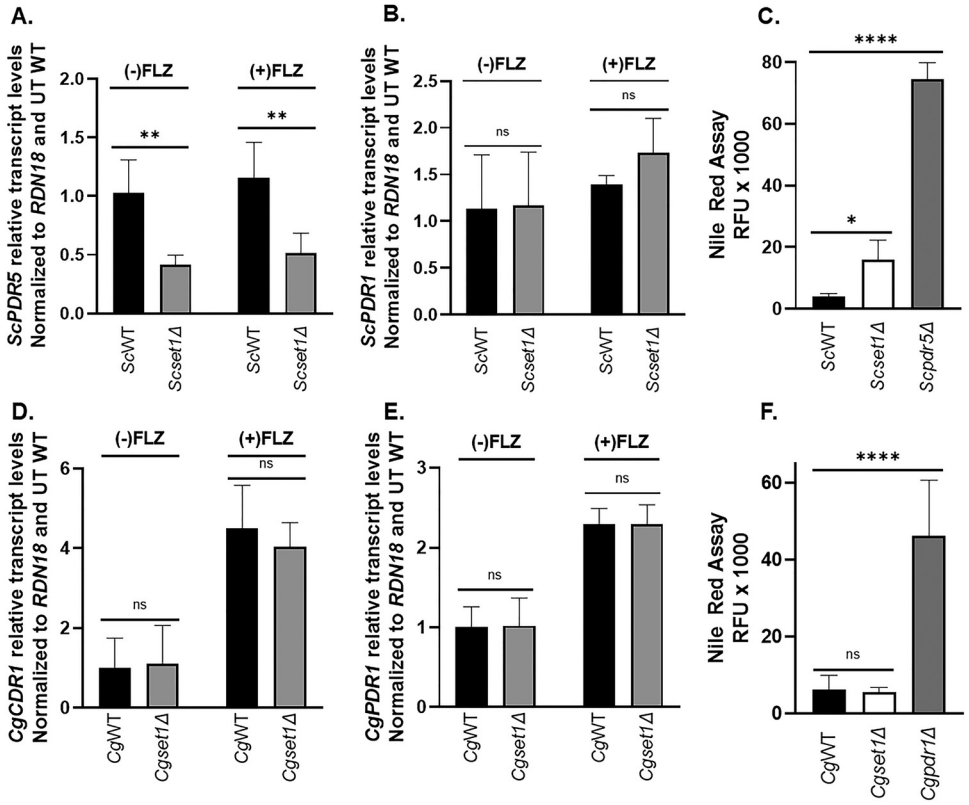

FIG 4 Drug efflux pump expression and drug efflux is altered in a *Scset1*Δ but not *Cgset1*Δ. (A and B; D and E) Expression of the indicated genes was determined in *Sc*WT, *Scset1*Δ, *Cg*WT, and *Cgset1*Δ strain cells treated with or without 64 μg/mL fluconazole for 3 h by qRT-PCR analysis. Gene expression analysis was set relative to the untreated wild type, and expression was normalized to *RDN18* mRNA levels. Data were analyzed from $\geq$3 biological replicates with three technical replicates each. Error bars represent the standard deviations (SD). (C and F) Red fluorescence units (RFU) were measured as output in a Nile red assay to determine the amount of drug efflux in the indicated strains with and without fluconazole. *Scpdr5*Δ and *Cgpdr1*Δ strains was used as controls. Data were analyzed from $\geq$3 biological replicates with three technical replicates each. Statistics were determined using the GraphPad Prism Student *t* test, version 9.2.0. ns, $P > 0.05$; *, $P < 0.05$; ****, $P < 0.0001$. Error bars represent SD.

compared to WT cells when grown with and without azoles (Fig. 4D and E). In addition, the transcript levels of other transporters *CgSNQ2*, *CgYOR1*, and *CgPDH1* were also not altered, but a decrease in *PDH1* transcripts was observed in *Cgset1*Δ cells upon azole treatment (see Fig. S2). However, previous studies have shown loss of *CgPDH1* alone is not sufficient to lead to azole sensitivity (47). To determine whether drug efflux was functional in *Cgset1*Δ cells, a Nile red fluorescence-based assay was performed. As a control, a *Cgpdr1*Δ strain was used (Fig. 4F). A *Cgpdr1*Δ strain is known to disrupt the expression of *CgCDR1* and subsequently prevent drug or Nile red efflux (15). To induce *CgCDR1* expression levels, *Cgset1*Δ and wild-type cells were treated with fluconazole. Although azole treatment did reduce the amount of Nile red in *Cg*WT cells compared to untreated cells (see Fig. S2E), there was no discernible difference in Nile red fluorescence between *Cgset1*Δ and *Cg*WT cells upon azole treatment (Fig. 4F). These data show that cells lacking *CgSET1* have similar efflux capabilities as *Cg*WT cells in the presence or absence of azole treatment. Our results suggest that the increase in azole susceptibility in a *Scset1*Δ strain is a consequence of altered drug efflux expression, whereas azole hypersensitivity in a *Cgset1*Δ strain is not due to altered expression or function of drug efflux pumps but mediated by a different mechanism.

Loss of *C. glabrata SET1* but not *S. cerevisiae SET1* leads to decreased expression of genes involved in the late ergosterol biosynthesis pathway when treated with fluconazole. Because drug efflux function or transcript levels were not disrupted in a *Cgset1*Δ strain, RNA sequencing analysis was used to provide insight into what gene pathway might be disrupted in the *Cgset1*Δ strain and explain why a loss of *SET1* alters

azole drug efficacy. *Cg*WT and *Cgset1*Δ strains were treated with 64 μg/mL fluconazole for 3 h in SC complete media, and RNA was extracted for RNA sequencing. Principal component analysis (PCA) and differentially expressed gene (DEG) analysis demonstrated by the volcano scatterplot (–$\log_2$ false discovery rate [FDR], *y*-axis) versus the fold change ([*x*-axis] of the DEGs) indicate that the untreated and treated *Cg*WT strain is substantially and statistically different from the untreated and treated *Cgset1*Δ (Fig. 5A). DESeq2 analysis was used to identify the differentially expressed genes (DEGs) using a FDR of 0.05 (see Table S6). From this analysis, a total of 2389 genes were differentially expressed in *Cgset1*Δ versus *Cg*WT strains under untreated conditions (Fig. 5B). Of 5,615 genes, 1,508 were differentially expressed under treated conditions, in which 800 (14.2%) genes were upregulated and 708 (12.6%) genes were downregulated in *Cgset1*Δ compared to *Cg*WT strains (Fig. 5C). After applying a 1.4-fold cutoff to the data, we observed 1,619 genes differentially expressed in the untreated *Cgset1*Δ versus *Cg*WT strains. In the treated strains, with a 1.4-fold cutoff, we observed 539 (9.6%) genes were downregulated in a *Cgset1*Δ versus *Cg*WT strains, and 623 (11.1%) genes were upregulated. These data show that *SET1* is important for maintaining proper gene expression in *C. glabrata*.

Because Set1-mediated histone H3K4 methylation is known to play a key role in gene activation, we focused our attention on genes downregulated in *Cgset1*Δ compared to *Cg*WT strains. For azole treated strains, GO Term Finder of the gene sets that were downregulated found significant GO terms involved in lipid, steroid, and sterol/ergosterol metabolism or biosynthesis (Fig. 5D; see also Table S7). For untreated strains, GO Term Finder identified significant GO terms involved in lipid metabolism but not steroid and sterol/ergosterol metabolism or biosynthesis. Interestingly, our data showed that 12 of the 12 genes involved in the late ergosterol biosynthesis pathway are downregulated 1.4-fold or more in a *Cgset1*Δ compared to *Cg*WT under azole-treated conditions (Fig. 5C; see also Fig. S4A and B and Table S6), whereas 5 of the 12 late pathway *CgERG* genes were downregulated in a *Cgset1*Δ compared to *Cg*WT strains under untreated conditions using a 1.4-fold difference as a cutoff (Fig. 5D; see also Table S6). Two of these differentially expressed genes—*ERG11*, the gene that encodes the target of azoles, and *ERG3*, the gene that encodes the enzyme responsible for production of a toxic sterol when cells are treated with azoles—are known to play roles in azole drug resistance in various *Candida* species (17, 19, 48–50).

To validate results seen in RNA sequencing analysis, *CgERG11* and *CgERG3* transcript levels were analyzed by qRT-PCR. Our analysis showed that upon azole treatment, *CgERG3* and *CgERG11* transcript levels are induced in a *Cg*WT strain (Fig. 5E and F), while loss of *CgSET1* prevented *Cg*WT induction of both *CgERG11* and *CgERG3* under azole treated conditions. Even though our untreated RNA sequencing data set did show minor changes in *CgERG3* and *CgERG11* transcript levels, we did not detect any significant changes between *Cgset1*Δ and *Cg*WT cells when grown under untreated standard log-phase conditions using qRT-PCR analysis (Fig. 5E and F). We also performed gene expression analysis to determine whether *CgERG* gene transcript induction still depended on *Cg*Set1 in saturated cultures. We show in both exponential and saturated cultures *Cg*Set1 is necessary for *CgERG3* and *CgERG11* induction upon azole treatment (Fig. 5E and F; see also Fig. S3A and B). Because *CgERG3* transcript levels were decreased, we do not anticipate azole sensitivity is due to an increase in toxic sterols but by the lack of induction of *CgERG11* and other *ERG* genes resulting in lower total cellular ergosterol levels (51, 52). In addition, we examined transcript levels of *ScERG11* in *Scset1*Δ cells. In contrast to *Cgset1*Δ, we observed a decrease in *ScERG11* transcripts under untreated conditions, but no difference was detected upon azole treatment (Fig. 5G). The *ScERG11* transcript data are consistent with what was previously published for *Scset1*Δ cells under untreated conditions (28). Altogether, our results show that the increase in azole susceptibility in a *Scset1*Δ strain is a consequence of decreased drug efflux expression, whereas azole hypersensitivity in a *Cgset1*Δ strain is not due to altered expression or function of drug efflux pumps but by decreased expression of genes needed for the late ergosterol pathway.

Set1-mediated histone H3K4 methylation is enriched on *ERG* gene chromatin and is required for azole induction of *ERG* genes. Because histone H3K4 trimethylation is associated with gene induction, we wanted to determine whether Set1 was directly

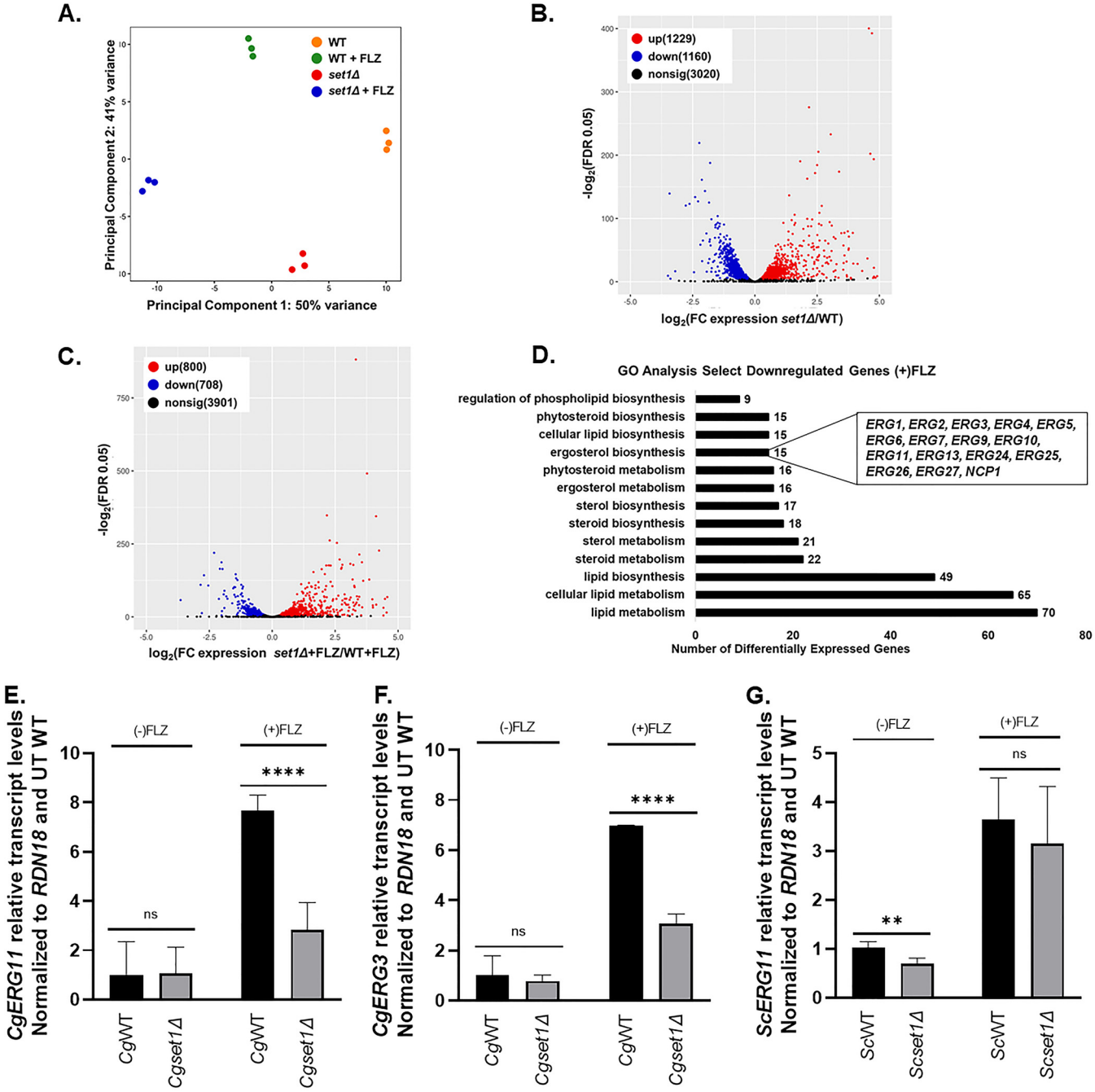

FIG 5 The deletion of *SET1* in *C. glabrata* alters global and local levels of gene expression under untreated and azole-treated conditions. The genomewide changes in gene expression under azoles were assessed using *C. glabrata* CBS138 (2001) WT and *set1*Δ strains. (A) PCA for WT and *set1*Δ azole-treated samples relative to WT untreated samples based on the counts per million. (B) Volcano plot showing the significance [$-\log_2$(FDR), *y* axis] versus the fold change (*x* axis) of the DEGs identified in the WT untreated samples relative to *set1*Δ untreated samples. (C) Volcano plot showing the significance [$-\log_2$(FDR), *y* axis] versus the fold change (*x* axis) of the DEGs identified in the *set1*Δ azole-treated samples relative to WT azole-treated samples. Genes with significant differential expression (FDR $<$ 0.05) in panels B and C are highlighted in red and blue for up- and downregulated genes, respectively. Black highlighted genes are considered nonsignificant. (D) Genes from the RNA-seq data set that were statistically significantly enriched (FDR $<$ 0.05) were used for GO term determination of Set1-dependent DEGs under azole conditions. Downregulated genes refer to the DEGs that are dependent on Set1 for activation either directly or indirectly. Significantly enriched groups of GO terms were identified as the DEGs from only *set1*Δ and WT azole-treated samples. (E to G) Expression of indicated genes was determined in WT and *set1*Δ strain cells in either *C. glabrata* or *S. cerevisiae* treated with 64 μg/mL fluconazole for 3 h by qRT-PCR analysis. Gene expression analysis was set relative to the untreated wild-type and expression was normalized to *RDN18* mRNA levels. Data were analyzed from ≥3 biological replicates with three technical replicates each. Statistics were determined using the GraphPad Prism Student *t* test, version 9.2.0. ****, $P < 0.0001$; **, $P < 0.01$; ns, $P > 0.05$. Error bars represent the SD.

catalyzing histone H3K4 methylation on chromatin at *ERG* loci. To determine whether histone H3K4 trimethylation was present at *CgERG11* and *CgERG3* chromatin, chromatin immunoprecipitation (ChIP) analysis was performed using histone H3K4 trimethyl-specific antibodies. As expected, histone H3K4 trimethylation is highly enriched at the 5′ ends of the open reading frame of *CgERG11* and *CgERG3* in untreated conditions and further enriched upon azole treatment corresponding to increased transcript levels of *CgERG11* and *CgERG3* in both exponential and saturated cell cultures (Fig. 6A and B; see also Fig. S3C and D).

To confirm that this was due to the methyltransferase activity of Set1, we performed qRT-PCR transcript analysis using the *Cg*2001HTU*set1*Δ strain expressing pGRB2.0 only, pGRB2.0-*CgSET1*, and pGRB2.0-*Cgset1H1048K*. *Cg*2001HTU expressing pGRB2.0 only was used as our WT control. As shown in Fig. 6C and D, pGRB2.0-*CgSET1* was able to induce *ERG11* and *ERG3* similar to WT cells under azole treatment, indicating that *SET1* expression could rescue the *ERG* gene expression in the *Cg*2001HTU*set1*Δ strain. This rescue of *ERG* gene expression was dependent on the catalytic activity of Set1 since expression of pGRB2.0-*Cgset1H1048K* did not restore *ERG* gene expression under azole treatment. In addition, it looked similar to the *Cg*2001HTU*set1*Δ strain expressing pGRB2.0, indicating that the catalytic activity of Set1 is required for azole gene induction. Altogether, these data show that Set1-mediated histone H3K4 methylation directly targets the chromatin of *ERG* genes, and this epigenetic modification is required for azole induction of *ERG* genes.

Hypersensitivity to azole drugs is suppressed by exogenous ergosterol for *C. glabrata set1*Δ but not for a *S. cerevisiae set1*Δ. Based on our expression analysis and decreased expression of 12 genes involved in the late ergosterol biosynthesis, we predict further decreased endogenous ergosterol levels in *C. glabrata* strains lacking *SET1*, thus making the *Cgset1*Δ more susceptible to azole drugs. To determine whether endogenous ergosterol levels are reduced in *Cgset1*Δ strains upon azole treatment, CgWT and *Cgset1*Δ strains were plated on SC media supplemented with exogenous ergosterol with or without fluconazole. In support of our hypothesis and gene expression data, exogenous ergosterol suppressed azole hypersensitivity of a *Cgset1*Δ strain when grown in the presence of fluconazole while *Cgset1*Δ grown without ergosterol remained hypersensitive to azoles (Fig. 7A). Because azole hypersensitivity in a *Scset1*Δ is a consequence of altered *ScPDR5* expression but not azole-induced gene expression, we hypothesized that exogenous sterols would not suppress azole hypersensitivity in the *Scset1*Δ. Based on serial-dilution spot assays, exogenous sterols did not suppress azole hypersensitivity in a *Scset1*Δ strain when grown in the presence of fluconazole and looked similar to *Scset1*Δ grown on SC media without ergosterol (Fig. 7B). A *Scpdr5*Δ was used as a control for azole hypersensitivity (see Fig. S2F).

To determine whether total ergosterol levels were altered in *Cgset1*Δ compared to *Cg*WT strains upon azole treatment, nonpolar lipids were extracted from *Cgset1*Δ and *Cg*WT strains with or without fluconazole treatment. Total ergosterol levels were determined using high performance liquid chromatography (HPLC) analysis and cholesterol was used as an internal control. Consistent with our gene expression analysis, HPLC analysis showed no difference in total ergosterol levels between untreated *Cgset1*Δ and *Cg*WT strains (Fig. 7C; see also Fig. S5), which is consistent with no changes in *ERG* gene expression under untreated conditions (Fig. 6). As expected, upon fluconazole treatment the ergosterol levels decreased for both *Cgset1*Δ and *Cg*WT (Fig. 7D; see also Fig. S5). However, the fluconazole-treated *Cgset1*Δ strain had ~50% less ergosterol than the fluconazole-treated *Cg*WT strain (Fig. 7E; see also Fig. S5), which is also consistent with our data showing that loss of *SET1* alters *ERG* gene expression only under treated conditions (Fig. 6). Our results suggest that the increased azole susceptibility of a Cg*set1*Δ strain is a consequence of defects in *ERG* gene expression resulting in decreases in ergosterol levels, whereas azole hypersensitivity in a *Scset1*Δ strain is a result of decreased efflux pump expression and not changes in ergosterol levels.

Loss of *SET1* in *C. glabrata* clinical isolates SM1 and resistant strain SM3 results in increased azole sensitivity and altered *CgERG11* gene expression. Because *C. glabrata* strains are genetically diverse in clinical isolates, we wanted to determine whether deleting *SET1* in *C. glabrata* clinical isolates altered azole susceptibility. To determine the impact of

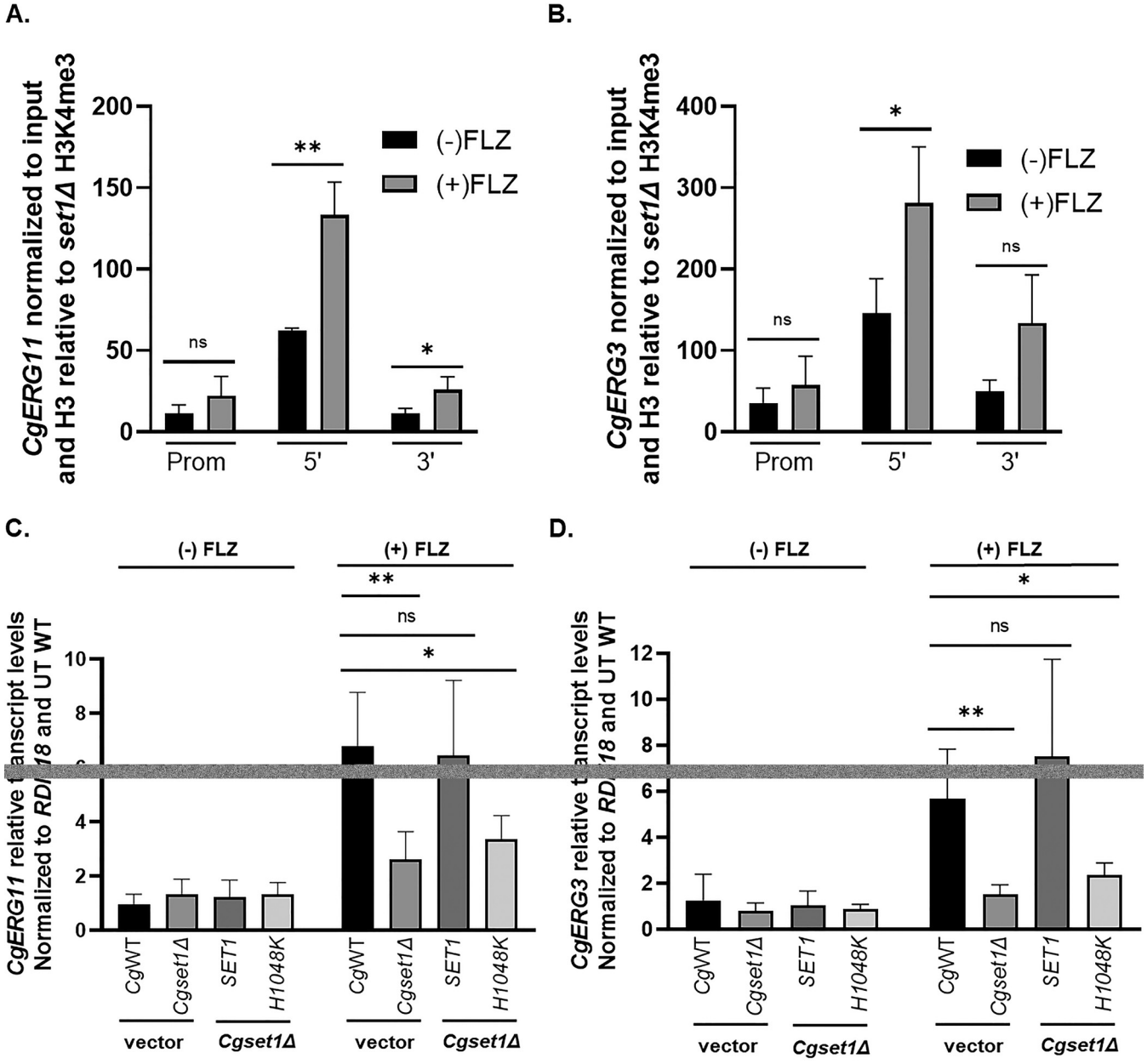

FIG 6 Set1-mediated histone H3K4 methylation is enriched on ERG gene chromatin and is required for azole induction of ERG genes. (A and B) ChIP analysis of histone H3K4 trimethylation levels at the promoter, 5′, and 3′ regions of *ERG11* and *ERG3* in a wild-type *C. glabrata* strain with or without 64 μg/mL fluconazole treatment. ChIP analysis was set relative to a *set1*Δ strain and normalized to histone H3 and DNA input levels. Data were analyzed from five biological replicates with three technical replicates each. *, $P < 0.05$. (C and D) Expression of indicated genes was determined in the indicated mutants treated with and without 64 μg/mL fluconazole for 3 h by qRT-PCR analysis. Gene expression analysis was set relative to the untreated wild-type containing an empty vector and expression was normalized to *RDN18* mRNA levels. Data were analyzed from ≥3 biological replicates with three technical replicates each. Statistics were determined using the GraphPad Prism Student *t* test, version 9.2.0. ns, $P > 0.05$; *, $P < 0.05$; **, $P < 0.01$. Error bars represent the SD.

deleting *SET1* in *C. glabrata* clinical isolates, *SET1* was deleted in the two characterized clinical isolates SM1 (fluconazole sensitive) and SM3 (fluconazole resistant) (53–55). Similar to the *Cgset1*Δ (Cg2001) strain, SM1 with *CgSET1* deleted showed increased susceptibility to azole drugs as shown by serial-dilution spot assays (Fig. 8A). Furthermore, deleting *CgSET1* from the clinically resistant SM3 strain, an isolate expressing a *CgPDR1* gain-of-function mutation resulting in an increase in *CgCDR1* expression, also resulted in increased susceptibility to azole treatment (Fig. 8B). Although deleting *SET1* in the SM3 strain does not restore SM3 strains to SM1 azole susceptible levels, this is somewhat expected because *Cg*2001*set1*Δ strains do not alter *PDR1* or *CDR1* expression. Furthermore, a SM1*set1*Δ*pdr1*Δ double deletion strain is more

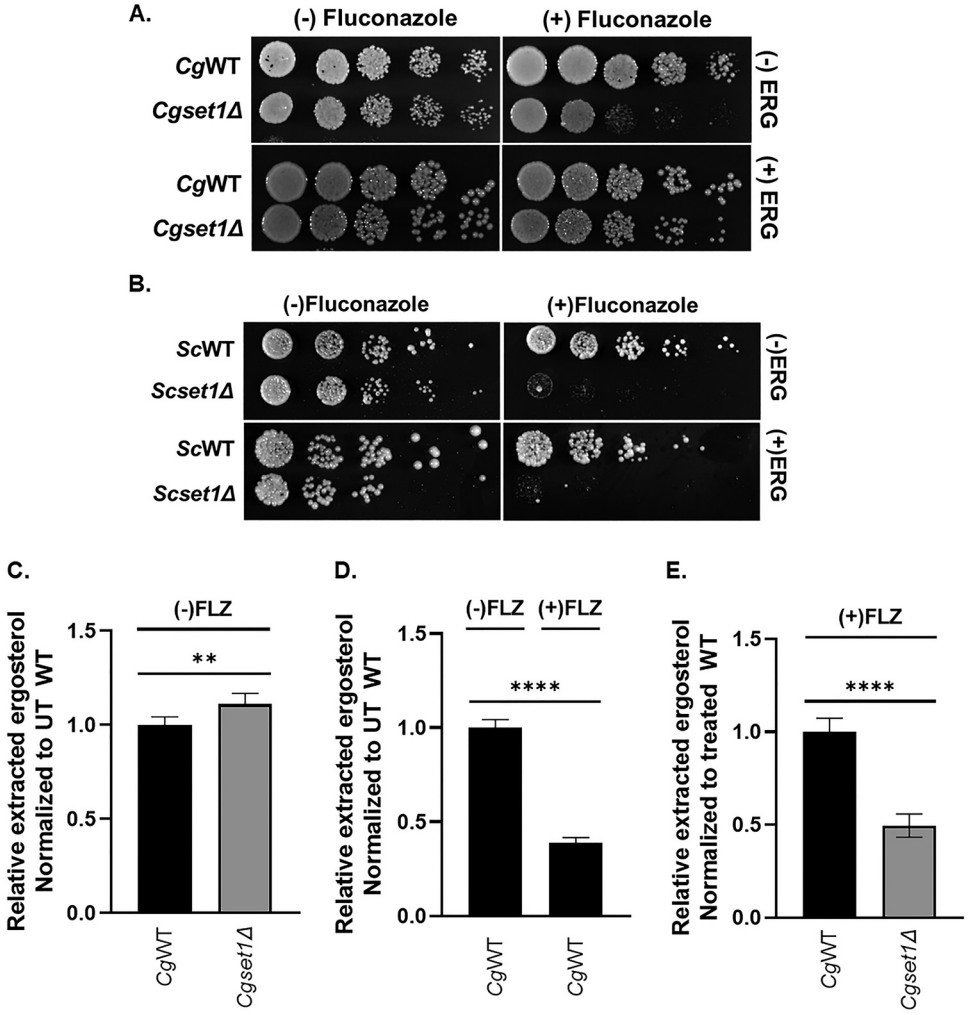

FIG 7 Loss of *SET1* in *C. glabrata* results in reduced endogenous ergosterol levels upon azole treatment. (A and B) Fivefold serial dilution spot assays of the indicated *S. cerevisiae* and *C. glabrata* strains were grown on SC plates with or without 8 or 32 μg/mL fluconazole, respectively, and 10 or 20 μg/mL ergosterol, respectively. (C to E) Total ergosterol was extracted from *C. glabrata* WT and *set1*Δ strains treated with or without 64 μg/mL fluconazole and analyzed by HPLC. The figure is depicted as a ratio of ergosterol to cholesterol and relative to untreated or treated WT. Data were generated from six biological replicates. Statistics were determined using the GraphPad Prism Student *t* test, version 9.2.0. ****, $P < 0.0001$; **, $P < 0.01$. Error bars represent the SD.

sensitive to fluconazole than either of the SM1*pdr1*Δ and SM1*set1*Δ when grown on plates with low concentrations of azole drugs (Fig. 8C). These genetic data are consistent with the idea that Set1 is altering another pathway and not drug efflux, which is consistent with our gene expression data. To determine whether SM1 and SM3 clinical isolates lacking *SET1* had similar gene expression defects to *Cg*2001*set1*Δ strains, drug efflux function and *CgERG11* expression were analyzed. The SM1*set1*Δ strain had similar Nile red fluorescence compared to SM1, indicating no defects in the function of drug efflux pumps (Fig. 8D). Although SM3*set1*Δ cells Nile red fluorescence was ~1.5-fold higher than SM3 cells, the overall drug efflux of both SM3 and SM3*set1*Δ strains were significantly more than SM1 and SM1*set1*Δ cells, a consequence of *CDR1* overexpression (Fig. 8D). Similar to *Cg*2001*set1*Δ strains, the SM1*set1*Δ and SM3*set1*Δ strains failed to induce *ERG11* expression under azole treatment (Fig. 8E and F).

DISCUSSION

In this study, we established that loss of Set1-mediated histone H3K4 methylation alters azole drug susceptibility in *S. cerevisiae* and *C. glabrata* by altering the expression of genes known to be involved in drug resistance. In *S. cerevisiae*, an azole-treated *Scset1*Δ

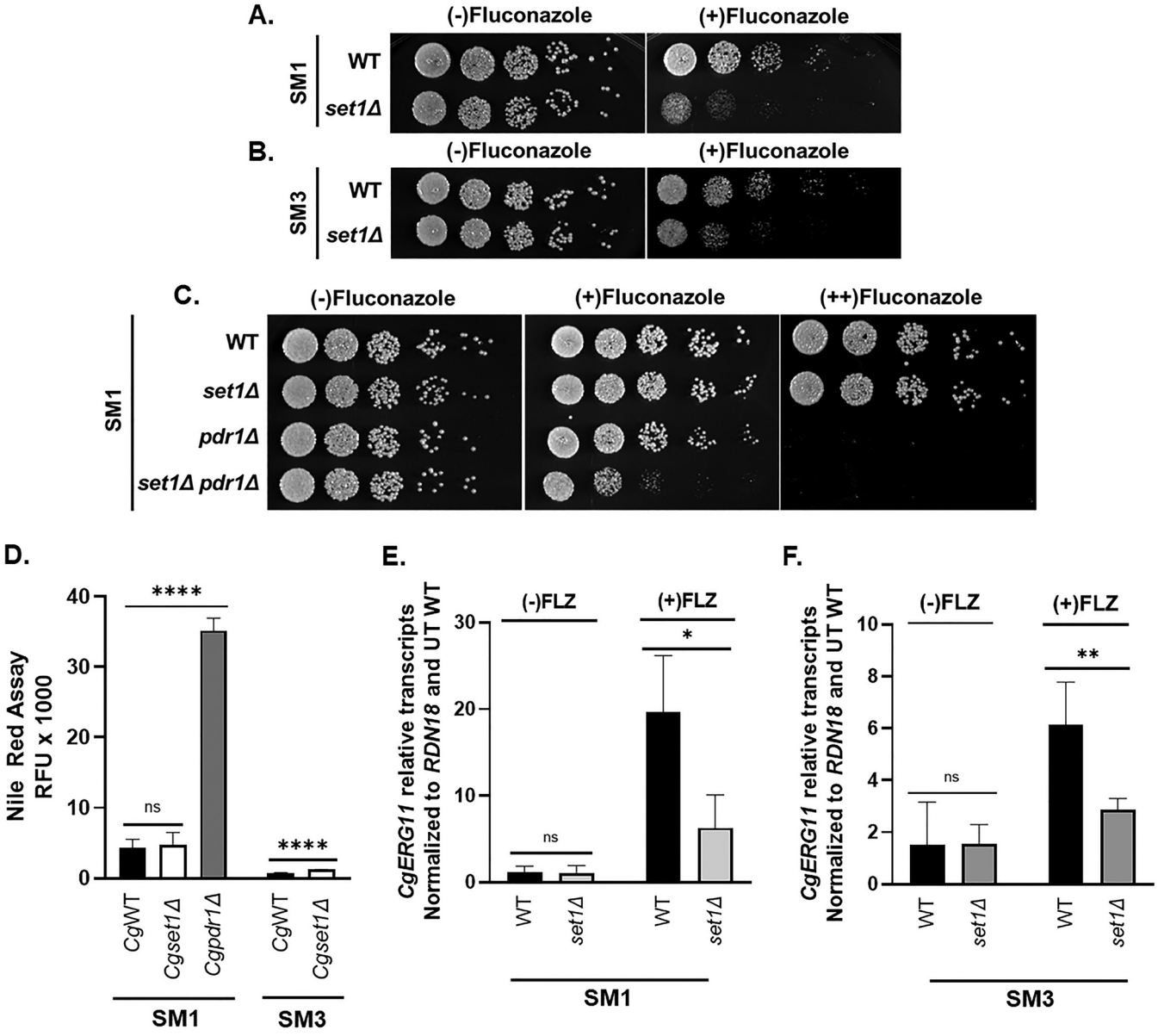

FIG 8 Loss of *SET1* in *C. glabrata* clinical isolates SM1 and resistant strain SM3 results in increased azole sensitivity. (A to C) Fivefold serial dilution spot assays of the indicated *C. glabrata* clinical isolates were grown on SC plates with or without fluconazole and/or 20 μg/mL ergosterol. (D) RFU were measured as output in a Nile red assay to determine the amount of drug efflux in the indicated SM1 and SM3 clinical isolates treated with 64 or 256 μg/mL fluconazole. A *Cgpdr1*Δ strain was used as a control. Data were analyzed from $\geq$ 3 biological replicates with three technical replicates each. (E and F) Expression of *ERG11* was determined from the indicated SM1 and SM3 clinical isolates treated with 64 and 256 μg/mL fluconazole, respectively, for 3 h by qRT-PCR analysis. Gene expression analysis was set relative to the untreated wild-type and expression was normalized to *RDN18* mRNA levels. Data were analyzed from $\geq$3 biological replicates with three technical replicates each. Error bars represent the SD. Statistics were determined using the GraphPad Prism Student *t* test, version 9.2.0. ns, $P > 0.05$; *, $P < 0.05$; **, $P < 0.01$; ****, $P < 0.0001$.

strain shows decreased expression of *ScPDR5* and consequently decreased drug efflux function, whereas the azole induction of *ScERG11* was similar to WT strains. In contrast, decreased azole susceptibility in a *Cgset1*Δ strain was caused by a failure to completely induce *CgERG* genes under azole treatment and not a consequence of altered *CgCDR1* and *CgPDR1* expression levels or ability to efflux drugs. This azole-induced gene expression in *C. glabrata* was dependent on *Cg*Set1 methyltransferase activity and correlated with gene-specific increases in histone H3K4 trimethylation on chromatin at *ERG* genes (see model, Fig. 9). Identifying and understanding how *SET1* and likely other epigenetic factors contribute to species-specific drug susceptibility will be important for the development of alternative drug targets that could be used in combinatorial therapy for treating patients with drug-resistant fungal infections.

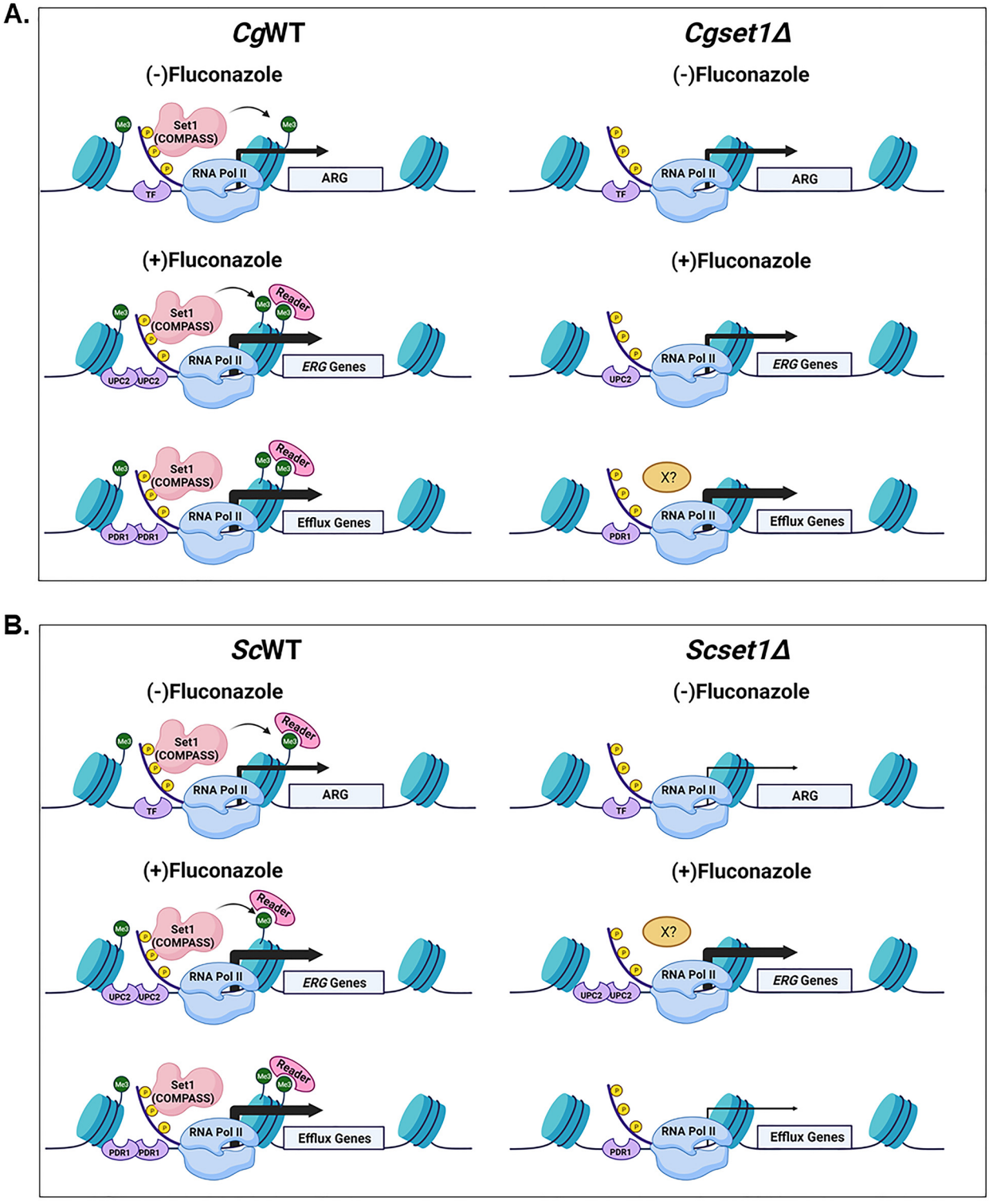

FIG 9 Model depicting the role of Set1 contributing to azole susceptibility in a species-specific manner (Biorender). (A and B) Transcriptional activation recruits TFs, RNA polymerase II, and the Set1 complex to increase histone H3K4 methylation and permit proper induction of gene expression. This increase in methylation could also recruitment other cofactors/epigenetic regulators (e.g., Set3 and/or SAGA complex) that contain "reader" domains that recognize and bind to the H3K4 methyl mark to help in expression. In addition, other factors ("X?") could be utilized to bypass the requirement of Set1. (A) In *C. glabrata*, azole-resistant genes (ARG) such as efflux pumps and *ERG* genes are induced upon azole treatment. In *Cgset1*Δ strains azole induction of *ERG* gene expression consequently ergosterol levels are decreased, but expression or function efflux pumps are not altered. (B) Under azole-treated conditions, efflux pump expression and function are decreased, but *ERG* gene expression is induced similar to WT levels.

Set1 is the catalytic subunit of a multisubunit protein complex called COMPASS that mono-, di-, and trimethylates histone H3K4. In this study, we show that *C. glabrata* Set1 is the sole histone H3K4 methyltransferase under log-phase growth conditions since deletion of *SET1* abolishes all forms of histone H3K4 methylation similar to what is seen in *S. cerevisiae* and *C. albicans* (30, 31). Additionally, deletion of the genes encoding *C. glabrata* COMPASS complex subunits Swd1 and Bre2 lead to a loss of histone H3K4 methylation similar to their *S. cerevisiae* counterparts (Fig. 2C) (33, 34, 36, 38). However, deleting *SPP1* in *C. glabrata* abolishes all histone H3K4 trimethylation and significantly reduces the levels of histone H3K4 mono- and dimethylation, which is in contrast to what is found in a *Scspp1*Δ strain where only histone H3K4 trimethylation is disrupted but retains WT levels of mono- and dimethylation (33, 34, 36, 38). We assume this difference in histone H3K4 methylation pattern is due to how *Cg*Spp1 assembles with the COMPASS complex allowing *Cg*Spp1 to have a greater impact on the overall catalytic activity of COMPASS. Interestingly, this pattern of methylation appears to correlate with sensitivity to azole drugs (Fig. 2B; see also Fig. S1A), where the *Scspp1*Δ strain grows more similarly to a WT strain than to the *Cgspp1*Δ strain when grown on azole-containing plates.

Our published observation has determined that *S. cerevisiae* and *C. glabrata* show hypersensitivity to azole drugs when lacking *SET1* (29). However, until this study, the mechanistic role of *SET1* under azole treatment in *S. cerevisiae* or *C. glabrata* has not been investigated. Our previous publication showed loss of *SET1* in *S. cerevisiae* altered expression of genes involved in early (e.g., *HMG1*) and late ergosterol biosynthesis (e.g., *ERG11*) under untreated log-phase growing conditions where decreased ergosterol levels were also observed (Fig. 5G) (28). In this study, we confirmed similar decreases in *ERG11* expression in the Sc*set1*Δ strain under untreated conditions. However, azole-induced *ERG11* expression was induced in the Sc*set1*Δ strain similar to that in the *Sc*WT strain. In addition, adding back exogenous ergosterol did not suppress azole sensitivity, indicating no defects in ergosterol levels under azole treatment. This lack of suppression was not due to aerobic exclusion of sterols of the Sc*set1*Δ strain because our previous publication showed that yeast lacking *SET1* can take up exogenous sterols under aerobic conditions (28). Intriguingly, brefeldin A (BFA) hypersensitivity of a Sc*set1*Δ strain is suppressed when treated with exogenous sterols indicating distinct differences between BFA treatment and azole treatment (28).

In contrast to the *Scset1*Δ strain, a *Cgset1*Δ strain showed changes in *ERG* gene expression under azole-treated conditions but not untreated conditions, suggesting that histone H3K4 methylation is needed for azole-induced gene induction and not basal level expression in *C. glabrata* (Fig. 5E and F). In addition, all 12 genes involved in the late ergosterol biosynthesis pathway were differentially expressed in the *Cgset1*Δ strain compared to the *Cg*WT strain, as well as three genes in the early pathways *ERG9*, *ERG10*, and *ERG13*, but not *HMG1*, indicating the importance of Set1 for this azole-induced pathway in *C. glabrata* but not in *S. cerevisiae*. We suspect that under azole treatment another epigenetic factor is contributing this role in *S. cerevisiae* and thus bypassing the requirement of Set1.

Although regulation of ergosterol biosynthesis has been shown to be coupled to expression of ABC transport genes such as *CgCDR1* and its transcription factor Pdr1 (56, 57), compensatory changes in *CgCDR1* and *CgPDR1* expression levels were not observed in a *Cgset1*Δ strain treated with azole drugs (Fig. 4D and E). Furthermore, when *SET1* was deleted in the clinical isolates SM1 (azole sensitive) and SM3 (azole resistant), both clinical isolates showed increased hypersensitivity to azole drugs compared to their respective isolates. Again, hypersensitivity was likely due to decreased *ERG* gene expression and not because of altered efflux pump function. Even though the SM3*set1*Δ strain is considered less resistant than SM3, the SM3*set1*Δ strain was not altered to that of SM1's sensitivity levels. We suspect this is because the loss of *CgSET1* does not significantly alter the expression of *CgPDR1* or *CgCDR1* expression levels to impact efflux and thus altering SM3's susceptibility but not resistance. More investigation will be needed to understand how *CDR1* and/or *PDR1* are epigenetically regulated in *C. glabrata* sensitive and clinically azole-resistant strains (26, 58).

Raman et al. reported that loss of *SET1* in *C. albicans* did not alter azole sensitivity but did decrease virulence in mice which was attributed to decreased epithelial adherence

(30). Interestingly, several genes encoding cell wall proteins and adhesion factors are also downregulated in a *Cgset1*Δ strain, as determined by RNA sequencing. In addition, *C. albicans* strains lacking *ERG11* or *ERG3* produce avirulent hyphae, decrease adherence to epithelial cells, and reduce virulence in oral mucosal infections and disseminated candidiasis (59–61). Based on these observations, we suspect that the loss of *CgSET1* could alter the virulence of *C. glabrata* under azole treatment. Additional studies will be needed to determine the *in vivo* contribution of *SET1* in *C. glabrata* and other *Candida* species.

Our data suggest that histone H3K4 methylation is an epigenetic mechanism to help induce *ERG* gene expression when *C. glabrata* strains are exposed to azole drugs. We propose histone H3K4 methylation and other epigenetic marks contribute to *C. glabrata*'s natural resistance to azole drugs. Interestingly, several histone deacetylases (HDACs), such as *Ca*Hda1, *Ca*Rpd3, and *Ca*Hos2, have been implemented in azole resistance in *C. albicans* (22, 23, 62–64). In addition, HDAC inhibitors have been shown to have a synergistic effect on cells when combined with azoles and echinocandins (62, 63, 65, 66). Interestingly, the treatment of *C. albicans* with trichostatin A (TSA) lacks the trailing effect observed in MIC assays when using azole drugs, and the lack of trailing effect was attributed to reduced *CDR* and *ERG* gene expression (63, 67). In a similar manner, the *Cgset1*Δ strain also lacked a trailing effect in our MIC assays (unpublished data), which we suspect is specifically due to the lack of azole-induced *ERG* gene expression since *CDR1* expression was not altered (Fig. 4D and 5). Furthermore, treatment of drug-resistant fungal pathogens, including various isolates of *C. glabrata*, with a Hos2 inhibitor MGCD290 showed synergy with azole drugs, which converted the MICs of azole treatment from resistant to susceptible (65). Because Hos2 is known to be a key component of the Set3 complex and the Set3 complex is recruited to chromatin via Set1-mediated histone H3K4 methylation (68, 69), it is likely MGCD290 is mediating its effect with azoles through inhibiting azole-induced *ERG* gene expression.

The occurrence of multidrug-resistant strains is increasing across all *Candida* species. In addition, with the development and identification of multidrug-resistant fungal species such as *C. auris*, a pathogen of urgent concern for the Centers for Disease Control and Prevention, it is imperative to find alternative treatment options. Our study, along with others, provides compelling evidence that epigenetic modifiers are playing key roles in altering fungal pathogenesis and drug susceptibility. Understanding these epigenetic events and the pathways they impact is needed to develop new drug therapies so that current and newly emerging multidrug-resistant fungal pathogens can be effectively treated.

MATERIALS AND METHODS

Plasmids and yeast strains. All plasmids and yeast strains are described in Tables S1 and S2. *C. glabrata* 2001 (CBS138, ATCC 2001) and *C. glabrata* 2001HTU (ATCC 200989) were purchased from the American Type Culture Collection (43). A genomic fragment containing the *CgSET1* promoter, 5′ UTR, open reading frame, and 3′ UTR was amplified by PCR and cloned into the pGRB2.0 plasmid. The pGRB2.0 plasmid was purchased from Addgene. Standard, site-directed mutagenesis was used to generate *Cgset1H1048K*. A 3×FLAG sequence was inserted between the endogenous promoter and ATG of the pGRB2.0-*CgSET1* and pGRB2.0-*Cgset1H1048K* using fusion-based PCR and restriction enzyme cloning. *Candida glabrata SET1*, *BRE2*, *SWD1*, *SPP1*, and *PDR1* genes were deleted via standard homologous recombination. Briefly, drug-resistant selection markers were PCR amplified with Ultramer DNA Oligos (IDT) using pAG32-HPHMX6 (hygromycin) or pAG25-NATMX6 (nourseothricin).

Serial-dilution spot and liquid growth assays. For serial-dilution spot assays, yeast strains were inoculated in SC media and grown to saturation overnight. Yeast strains were diluted to an optical density at 600 nm (OD_{600}) of 0.1 and grown in SC media to log phase with shaking at 30°C. The indicated strains were spotted in 5-fold dilutions starting at an OD_{600} of 0.01 on untreated SC plates or plates containing 16, 32, or 64 μg/mL fluconazole (Sigma-Aldrich, St. Louis, MO). Plates were grown at 30° for 1 to 3 days. For growth assays, the indicated yeast strains were inoculated in SC media and grown to saturation overnight. Yeast strains were diluted to an OD_{600} of 0.1 and grown in SC media to log phase with shaking at 30°C. The indicated strains were diluted to an OD_{600} of 0.0001 in 100 μL SC media. Cells were left untreated or treated with 64 μg/mL fluconazole and grown for 50 h with shaking at 30°C. The cell density OD_{600} was determined every 1 h using the Bio-Tek Synergy 4 multimode plate reader.

Cell extract and Western blot analysis. Whole-cell extraction and Western blot analysis to detect histone modifications were performed as previously described (36, 70). Histone H3K4 methylation-specific antibodies were used as previously described: H3K4me1 (Upstate, catalog no. 07-436; 1:2,500), H3K4me2 (Upstate, catalog no. 07-030; 1:10,000), and H3K4me3 (Active motif 39159, 1:100,000) (28, 71). Histone H3 antibodies were used as our loading control (Abcam, catalog no. ab1791; 1:10,000).

RNA sequencing analysis. The CBS138 *Cg*2001 WT and *set1*Δ strains were inoculated in SC media and grown to saturation overnight. Cells were diluted to an OD_{600} of 0.1 and recovered to log phase for

3 h with shaking at 30°C. Prior to treatment, cells were collected for the untreated sample and zero time point. Cultures were treated at an OD_{600} of 0.2 with 64 μg/mL fluconazole (Sigma-Aldrich) dissolved in dimethyl sulfoxide as previously described (72). Cells were collected after 3 h. The total RNA of three biological replicates for each condition and sample was isolated by standard acid phenol purification and treated with DNase (Ambion), and the total RNA was purified using standard acid phenol purification. The quality of the RNA was tested using an Agilent Bioanalyzer 2100 using a High Sensitivity DNA Chip. The cDNA library was prepared by the Purdue Genomics Facility using the TruSeq stranded kit with poly(A) selection (Illumina) according to the manufacturer's instructions. The software Trimmomatic v.0.39 was used to trim reads, removing adapters and low-quality bases (73). STAR v.2.5.4b was used to align reads to the *C. glabrata* CBS138 reference genome, version s02-m07-r23 (74). One mismatch was allowed per read. HTSeq v.0.6.1 was used to generate the gene count matrix on "intersection-nonempty" mode (75). R version 3.5.1 and Bioconductor release 3.6 were used to perform all statistical analyses on the RNA-seq data. The intersection of genes identified as statistically significantly differentially expressed with a Benjamini-Hochberg-corrected FDR of $<$5% by DESeq2 v.1.18.0 was used in downstream analyses (76, 77).

Quantitative real-time PCR analysis. RNA was isolated from cells by standard acid phenol purification. Reverse transcription was performed using an All-in-One 5$\times$ RT Mastermix kit (ABM, Richmond, Canada). Primer Express 3.0 software was used for designing primers, and qRT-PCR was performed as previously described (28, 78, 79). At least three biological replicates, including three technical replicates, were performed for all samples. Data were analyzed using the comparative C_T method ($2^{-\Delta\Delta CT}$), where *RDN18* (18S rRNA) was used as an internal control. All samples were normalized to an untreated, untagged WT strain.

MIC assay. MIC assays were performed based on a modified version of the CLSI method for testing yeast, 3rd edition (80). Briefly, yeast strains were inoculated in SC media and grown to saturation overnight. The indicated strains were diluted to an OD_{600} of 0.003 in in SC or RPMI media. Cells were mixed with fluconazole (Cayman Chemical) for a final volume of 100 μL per well in a 96-well polystyrene microplate, with concentrations of fluconazole ranging from 0 to 256 μg/mL. Plates were incubated at 35°C, and MICs were recorded at 24 h. MICs were determined visually where $>$90% of growth was inhibited.

Nile red assay. Fluorescence-based Nile red assays were performed as previously described (45). Briefly, cells were grown overnight in SC media to saturation. Cells were back diluted to an OD_{600} of 0.1 and grown at 30°C for 6 h. Cells were collected and then washed with phosphate-buffered saline (PBS) twice and incubated in 1.5 mL of PBS plus 2% glucose for 1 h. Next, 2.87 μL of a 1-mg/mL stock of Nile red (Sigma) was added to each sample, followed by incubation at 30°C shaking for an additional 30 min. Samples were washed twice with PBS and placed in triplicate in a black 96-well flat-bottomed polystyrene microplate. Fluorescence was detected using a Bio-Tek Synergy 4 multimode plate reader using an excitation wavelength of 553 nm and an emission wavelength of 636 nm.

Chromatin immunoprecipitation. ZipChIP was performed as previously described (71). Briefly, 50-mL cultures were grown to log phase (OD_{600} of 0.6) in SC complete media at 30°C shaking. Treated cells were dosed with 64 μg/mL fluconazole (Cayman Chemical) at an OD_{600} of 0.2 for 3 h. In addition, cultures were grown to saturation, back diluted to an OD_{600} of 0.6, treated with 64 μg/mL fluconazole for 3 h, and collected. Cells were formaldehyde cross-linked and harvested as previously described (71). Cell lysates were precleared with 5 μL of unbound protein G-magnetic beads for 30 min with rotation at 4°C. A total of 12.5 μL of precleared lysate was immunoprecipitated with 10 μL of protein G-magnetic beads (10004D; Life Technologies) conjugated to 1 μL of histone H3K4me3 antibody (Millipore, catalog no. 07-473) or histone H3 antibody (Abcam, catalog no. ab1791). Probe sets used in qRT-PCR are described in Table S5.

Ergosterol extraction. Ergosterol extraction was performed previously described (28). Cultures were grown overnight in SC minimal media. Saturated cultures were backdiluted to an OD_{600} of 0.1 and were grown at 30°C to log phase (OD_{600} 0.6) with or without 64 μg/mL fluconazole treatment. Sterols were extracted from yeast using 4 M potassium hydroxide in 70% (vol/vol) ethanol at 85°C for 1 h. After extraction, nonpolar lipids were separated using methanol two times. Nonpolar sterols were crystallized after evaporation of the N-hexane and dissolved in 100% methanol. Samples were then analyzed by HPLC using a C_{18} column with the flow rate set at 1 mL/min of 100% methanol. Ergosterol was detected at 280 nm. Cholesterol was added as an extraction internal control and was detected at 210 nm.

SUPPLEMENTAL MATERIAL

Supplemental material is available online only.

SUPPLEMENTAL FILE 1, PDF file, 1.1 MB.

SUPPLEMENTAL FILE 2, XLSX file, 0.2 MB.

SUPPLEMENTAL FILE 3, XLSX file, 0.02 MB.

ACKNOWLEDGMENTS

This study was supported by grants from the National Institutes of Health to S.D.B. (AI136995), the Purdue Department of Biochemistry Bird Stair Fellowship (to K.M.B.), Purdue Center for Cancer Research (grant P30CA023168: DNA Sequencing Shared Resource and Collaborative Core for Cancer Bioinformatics at Purdue), and The Walther Cancer Foundation and the IU Simon Cancer Center (grant P30CA082709). Additional funding support was provided by the NIFA 1007570 (S.D.B.).

We thank the Purdue Bioinformatics Core for their pipelines and bioinformatics software and P. David Rogers, St. Jude Children's Research Hospital, for the *C. glabrata* SM1 and SM3 clinical isolates.

REFERENCES

1. Wisplinghoff H, Bischoff T, Tallent SM, Seifert H, Wenzel RP, Edmond MB. 2004. Nosocomial bloodstream infections in US hospitals: analysis of 24,179 cases from a prospective nationwide surveillance study. Clin Infect Dis 39:309–317. https://doi.org/10.1086/421946.
2. Wisplinghoff H, Ebbers J, Geurtz L, Stefanik D, Major Y, Edmond MB, Wenzel RP, Seifert H. 2014. Nosocomial bloodstream infections due to *Candida* spp. in the USA: species distribution, clinical features, and antifungal susceptibilities. Int J Antimicrob Agents 43:78–81. https://doi.org/10.1016/j.ijantimicag.2013.09.005.
3. Chen S, Slavin M, Nguyen Q, Marriott D, Playford EG, Ellis D, Sorrell T, Study AC, The Australian Candidemia Study. 2006. Active surveillance for candidemia. Emerg Infect Dis 12:1508–1516. https://doi.org/10.3201/eid1210.060389.
4. Chouhan S, Kallianpur S, Prabhu KT, Tijare M, Kasetty S, Gupta S. 2019. Candidal prevalence in diabetics and its species identification. Int J Appl Basic Med Res 9:49–54. https://doi.org/10.4103/ijabmr.IJABMR_259_18.
5. Khatib R, Johnson LB, Fakih MG, Riederer K, Briski L. 2016. Current trends in candidemia and species distribution among adults: *Candida glabrata* surpasses *C. albicans* in diabetic patients and abdominal sources. Mycoses 59:781–786. https://doi.org/10.1111/myc.12531.
6. Hachem R, Hanna H, Kontoyiannis D, Jiang Y, Raad I. 2008. The changing epidemiology of invasive candidiasis: *Candida glabrata* and *Candida krusei* as the leading causes of candidemia in hematologic malignancy. Cancer 112:2493–2499. https://doi.org/10.1002/cncr.23466.
7. Vermitsky JP, Edlind TD. 2004. Azole resistance in *Candida glabrata*: coordinate upregulation of multidrug transporters and evidence for a Pdr1-like transcription factor. Antimicrob Agents Chemother 48:3773–3781. https://doi.org/10.1128/AAC.48.10.3773-3781.2004.
8. Pelz RK, Lipsett PA, Swoboda SM, Diener-West M, Powe NR, Brower RG, Perl TM, Hammond JM, Hendrix CW. 2000. *Candida* infections: outcome and attributable ICU costs in critically ill patients. J Intensive Care Med 15:255–261. https://doi.org/10.1046/j.1525-1489.2000.00255.x.
9. Rentz AM, Halpern MT, Bowden R. 1998. The impact of candidemia on length of hospital stay, outcome, and overall cost of illness. Clin Infect Dis 27:781–788. https://doi.org/10.1086/514955.
10. Pfaller MA, Jones RN, Messer SA, Edmond MB, Wenzel RP, Grp SP. 1998. National surveillance of nosocomial blood stream infection due to species of *Candida* other than *Candida albicans*: frequency of occurrence and antifungal susceptibility in the SCOPE program. Diagn Microbiol Infect Dis 30:121–129. https://doi.org/10.1016/S0732-8893(97)00192-2.
11. Pappas PG, Kauffman CA, Andes DR, Clancy CJ, Marr KA, Ostrosky-Zeichner L, Reboli AC, Schuster MG, Vazquez JA, Walsh TJ, Zaoutis TE, Sobel JD. 2016. Clinical practice guideline for the management of candidiasis: 2016 update by the Infectious Diseases Society of America. Clin Infect Dis 62:e1-50–50. https://doi.org/10.1093/cid/civ933.
12. Whaley SG, Rogers PD. 2016. Azole resistance in *Candida glabrata*. Curr Infect Dis Rep 18:41. https://doi.org/10.1007/s11908-016-0554-5.
13. Tscherner M, Schwarzmüller T, Kuchler K. 2011. Pathogenesis and antifungal drug resistance of the human fungal pathogen *Candida glabrata*. Pharmaceuticals (Basel) 4:169–186. https://doi.org/10.3390/ph4010169.
14. Tsai HF, Krol AA, Sarti KE, Bennett JE. 2006. *Candida glabrata* PDR1, a transcriptional regulator of a pleiotropic drug resistance network, mediates azole resistance in clinical isolates and petite mutants. Antimicrob Agents Chemother 50:1384–1392. https://doi.org/10.1128/AAC.50.4.1384-1392.2006.
15. Galkina KV, Okamoto M, Chibana H, Knorre DA, Kajiwara S. 2020. Deletion of CDR1 reveals redox regulation of pleiotropic drug resistance in *Candida glabrata*. Biochimie 170:49–56. https://doi.org/10.1016/j.biochi.2019.12.002.
16. Warrilow AG, Mullins JG, Hull CM, Parker JE, Lamb DC, Kelly DE, Kelly SL. 2012. S279 point mutations in *Candida albicans* sterol 14-α demethylase (CYP51) reduce *in vitro* inhibition by fluconazole. Antimicrob Agents Chemother 56:2099–2107. https://doi.org/10.1128/AAC.05389-11.
17. Flowers SA, Barker KS, Berkow EL, Toner G, Chadwick SG, Gygax SE, Morschhäuser J, Rogers PD. 2012. Gain-of-function mutations in UPC2 are a frequent cause of ERG11 upregulation in azole-resistant clinical isolates of *Candida albicans*. Eukaryot Cell 11:1289–1299. https://doi.org/10.1128/EC.00215-12.
18. Sanguinetti M, Posteraro B, Fiori B, Ranno S, Torelli R, Fadda G. 2005. Mechanisms of azole resistance in clinical isolates of *Candida glabrata* collected during a hospital survey of antifungal resistance. Antimicrob Agents Chemother 49:668–679. https://doi.org/10.1128/AAC.49.2.668-679.2005.
19. Whaley SG, Berkow EL, Rybak JM, Nishimoto AT, Barker KS, Rogers PD. 2016. Azole antifungal resistance in *Candida albicans* and emerging non-albicans *Candida* species. Front Microbiol 7:2173. https://doi.org/10.3389/fmicb.2016.02173.
20. Sanglard D, Ischer F, Calabrese D, Majcherczyk PA, Bille J. 1999. The ATP binding cassette transporter gene CgCDR1 from *Candida glabrata are* involved in the resistance of clinical isolates to azole antifungal agents. Antimicrob Agents Chemother 43:2753–2765. https://doi.org/10.1128/AAC.43.11.2753.
21. O'Kane CJ, Hyland EM. 2019. Yeast epigenetics: the inheritance of histone modification states. Biosci Rep 39:BSR20182006. https://doi.org/10.1042/BSR20182006.
22. Li X, Cai Q, Mei H, Zhou X, Shen Y, Li D, Liu W. 2015. The Rpd3/Hda1 family of histone deacetylases regulates azole resistance in *Candida albicans*. J Antimicrob Chemother 70:1993–2003. https://doi.org/10.1093/jac/dkv070.
23. Robbins N, Leach MD, Cowen LE. 2012. Lysine deacetylases Hda1 and Rpd3 regulate Hsp90 function thereby governing fungal drug resistance. Cell Rep 2:878–888. https://doi.org/10.1016/j.celrep.2012.08.035.
24. Shivarathri R, Tscherner M, Zwolanek F, Singh NK, Chauhan N, Kuchler K. 2019. The fungal histone acetyl transferase Gcn5 controls virulence of the human pathogen *Candida albicans* through multiple pathways. Sci Rep 9:9445. https://doi.org/10.1038/s41598-019-45817-5.
25. Lopes da Rosa J, Boyartchuk VL, Zhu LJ, Kaufman PD. 2010. Histone acetyltransferase Rtt109 is required for *Candida albicans* pathogenesis. Proc Natl Acad Sci U S A 107:1594–1599. https://doi.org/10.1073/pnas.0912427107.
26. Orta-Zavalza E, Guerrero-Serrano G, Gutierrez-Escobedo G, Canas-Villamar I, Juarez-Cepeda J, Castano I, De Las Penas A. 2013. Local silencing controls the oxidative stress response and the multidrug resistance in *Candida glabrata*. Mol Microbiol 88:1135–1148. https://doi.org/10.1111/mmi.12247.
27. Filler EE, Liu Y, Solis NV, Wang L, Diaz LF, Edwards JE, Filler SG, Yeaman MR. 2021. Identification of *Candida glabrata* transcriptional regulators that govern stress resistance and virulence. Infect Immun 89:e00146-20. https://doi.org/10.1128/IAI.00146-20.
28. South PF, Harmeyer KM, Serratore ND, Briggs SD. 2013. H3K4 methyltransferase Set1 is involved in maintenance of ergosterol homeostasis and resistance to brefeldin A. Proc Natl Acad Sci U S A 10:E1016–E1025.
29. Serratore ND, Baker KM, Macadlo LA, Gress AR, Powers BL, Atallah N, Westerhouse KM, Hall MC, Weake VM, Briggs SD. 2018. A novel sterol-signaling pathway governs azole antifungal drug resistance and hypoxic gene repression in *Saccharomyces cerevisiae*. Genetics 208:1037–1055. https://doi.org/10.1534/genetics.117.300554.
30. Raman S, Nguyen M, Zhang Z, Cheng S, Jia H, Weisner N, Iczkowski K, Clancy C. 2006. *Candida albicans* SET1 encodes a histone 3 lysine 4 methyltransferase that contributes to the pathogenesis of invasive candidiasis. Mol Microbiol 60:697–709. https://doi.org/10.1111/j.1365-2958.2006.05121.x.
31. Briggs SD, Bryk M, Strahl BD, Cheung WL, Davie JK, Dent SY, Winston F, Allis CD. 2001. Histone H3 lysine 4 methylation is mediated by Set1 and required for cell growth and rDNA silencing in *Saccharomyces cerevisiae*. Genes Dev 15:3286–3295. https://doi.org/10.1101/gad.940201.
32. Roguev A, Schaft D, Shevchenko A, Pijnappel WW, Wilm M, Aasland R, Stewart AF. 2001. The *Saccharomyces cerevisiae* Set1 complex includes an Ash2 homologue and methylates histone 3 lysine 4. EMBO J 20:7137–7148. https://doi.org/10.1093/emboj/20.24.7137.
33. Nagy PL, Griesenbeck J, Kornberg RD, Cleary ML. 2002. A trithorax-group complex purified from *Saccharomyces cerevisiae* is required for methylation of histone H3. Proc Natl Acad Sci U S A 99:90–94. https://doi.org/10.1073/pnas.221596698.
34. Dehe PM, Dichtl B, Schaft D, Roguev A, Pamblanco M, Lebrun R, Rodriguez-Gil A, Mkandawire M, Landsberg K, Shevchenko A, Shevchenko A, Rosaleny LE, Tordera V, Chavez S, Stewart AF, Geli V. 2006. Protein interactions within the Set1 complex and their roles in the regulation of histone 3-lysine 4-methylation. J Biol Chem 281:35404–35412. https://doi.org/10.1074/jbc.M603099200.
35. Takahashi YH, Westfield GH, Oleskie AN, Trievel RC, Shilatifard A, Skiniotis G. 2011. Structural analysis of the core COMPASS family of histone H3K4 methylases from yeast to human. Proc Natl Acad Sci U S A 108:20526–20531. https://doi.org/10.1073/pnas.1109360108.

36. Mersman DP, Du HN, Fingerman IM, South PF, Briggs SD. 2012. Charge-based interaction conserved within histone H3 lysine 4 (H3K4) methyltransferase complexes is needed for protein stability, histone methylation, and gene expression. J Biol Chem 287:2652–2665. https://doi.org/10.1074/jbc.M111.280867.
37. Shilatifard A. 2012. The COMPASS family of histone H3K4 methylases: mechanisms of regulation in development and disease pathogenesis. Annu Rev Biochem 81:65–95. https://doi.org/10.1146/annurev-biochem-051710-134100.
38. Mueller JE, Canze M, Bryk M. 2006. The requirements for COMPASS and Paf1 in transcriptional silencing and methylation of histone H3 in *Saccharomyces cerevisiae*. Genetics 173:557–567. https://doi.org/10.1534/genetics.106.055400.
39. Eissenberg JC, Shilatifard A. 2010. Histone H3 lysine 4 (H3K4) methylation in development and differentiation. Dev Biol 339:240–249. https://doi.org/10.1016/j.ydbio.2009.08.017.
40. Zordan RE, Ren Y, Pan S-J, Rotondo G, De Las Peñas A, Iluore J, Cormack BP. 2013. Expression plasmids for use in *Candida glabrata*. G3 (Bethesda) 3:1675–1686. https://doi.org/10.1534/g3.113.006908.
41. Schlichter A, Cairns BR. 2005. Histone trimethylation by Set1 is coordinated by the RRM, autoinhibitory, and catalytic domains. EMBO J 24:1222–1231. https://doi.org/10.1038/sj.emboj.7600607.
42. Soares LM, Radman-Livaja M, Lin SG, Rando OJ, Buratowski S. 2014. Feedback control of Set1 protein levels is important for proper H3K4 methylation patterns. Cell Rep 6:961–972. https://doi.org/10.1016/j.celrep.2014.02.017.
43. Kitada K, Yamaguchi E, Arisawa M. 1995. Cloning of the *Candida glabrata* TRP1 and HIS3 genes, and construction of their disruptant strains by sequential integrative transformation. Gene 165:203–206. https://doi.org/10.1016/0378-1119(95)00552-h.
44. Vermitsky JP, Earhart KD, Smith WL, Homayouni R, Edlind TD, Rogers PD. 2006. Pdr1 regulates multidrug resistance in *Candida glabrata*: gene disruption and genome-wide expression studies. Mol Microbiol 61:704–722. https://doi.org/10.1111/j.1365-2958.2006.05235.x.
45. Tsao S, Weber S, Cameron C, Nehme D, Ahmadzadeh E, Raymond M. 2016. Positive regulation of the *Candida albicans* multidrug efflux pump Cdr1p function by phosphorylation of its N-terminal extension. J Antimicrob Chemother 71:3125–3134. https://doi.org/10.1093/jac/dkw252.
46. Ivnitski-Steele I, Holmes A, Lamping E, Monk B, Cannon R, Sklar L. 2009. Identification of Nile red as a fluorescent substrate of the *Candida albicans* ATP-binding cassette transporters Cdr1p and Cdr2p and the major facilitator superfamily transporter Mdr1p. Anal Biochem 394:87–91. https://doi.org/10.1016/j.ab.2009.07.001.
47. Whaley SG, Zhang Q, Caudle KE, Rogers PD. 2018. Relative contribution of the ABC transporters Cdr1, Pdh1, and Snq2 to azole resistance in *Candida glabrata*. Antimicrob Agents Chemother 62:e01070-18. https://doi.org/10.1128/AAC.01070-18.
48. Flowers SA, Colon B, Whaley SG, Schuler MA, Rogers PD. 2015. Contribution of clinically derived mutations in ERG11 to azole resistance in *Candida albicans*. Antimicrob Agents Chemother 59:450–460. https://doi.org/10.1128/AAC.03470-14.
49. Kelly SL, Lamb DC, Kelly DE. 1997. Sterol 22-desaturase, cytochrome P45061, possesses activity in xenobiotic metabolism. FEBS Lett 412:233–235. https://doi.org/10.1016/s0014-5793(97)00785-0.
50. Morio F, Pagniez F, Lacroix C, Miegeville M, Le Pape P. 2012. Amino acid substitutions in the *Candida albicans* sterol Δ5,6-desaturase (Erg3p) confer azole resistance: characterization of two novel mutants with impaired virulence. J Antimicrob Chemother 67:2131–2138. https://doi.org/10.1093/jac/dks186.
51. Kelly SL, Lamb DC, Kelly DE, Manning NJ, Loeffler J, Hebart H, Schumacher U, Einsele H. 1997. Resistance to fluconazole and cross-resistance to amphotericin B in *Candida albicans* from AIDS patients caused by defective sterol Δ5,6-desaturation. FEBS Lett 400:80–82. https://doi.org/10.1016/s0014-5793(96)01360-9.
52. Watson PF, Rose ME, Ellis SW, England H, Kelly SL. 1989. Defective sterol C5-6 desaturation and azole resistance: a new hypothesis for the mode of action of azole antifungals. Biochem Biophys Res Commun 164:1170–1175. https://doi.org/10.1016/0006-291x(89)91792-0.
53. Caudle KE, Barker KS, Wiederhold NP, Xu L, Homayouni R, Rogers PD. 2011. Genomewide expression profile analysis of the *Candida glabrata* Pdr1 regulon. Eukaryot Cell 10:373–383. https://doi.org/10.1128/EC.00073-10.
54. Magill SS, Shields C, Sears CL, Choti M, Merz WG. 2006. Triazole cross-resistance among *Candida* spp.: case report, occurrence among bloodstream isolates, and implications for antifungal therapy. J Clin Microbiol 44:529–535. https://doi.org/10.1128/JCM.44.2.529-535.2006.
55. Whaley SG, Caudle KE, Vermitsky JP, Chadwick SG, Toner G, Barker KS, Gygax SE, Rogers PD. 2014. UPC2A is required for high-level azole antifungal resistance in *Candida glabrata*. Antimicrob Agents Chemother 58:4543–4554. https://doi.org/10.1128/AAC.02217-13.
56. Vu B, Thomas G, Moye-Rowley W. 2019. Evidence that ergosterol biosynthesis modulates activity of the Pdr1 transcription factor in *Candida glabrata*. mBio 10:e00934-19. https://doi.org/10.1128/mBio.00934-19.
57. Moye-Rowley WS. 2020. Linkage between genes involved in azole resistance and ergosterol biosynthesis. PLoS Pathog 16:e1008819. https://doi.org/10.1371/journal.ppat.1008819.
58. Yu SJ, Chang YL, Chen YL. 2018. Deletion of ADA2 increases antifungal drug susceptibility and virulence in *Candida glabrata*. Antimicrob Agents Chemother 62:e01924-17. https://doi.org/10.1128/AAC.01924-17.
59. Zhou Y, Liao M, Zhu C, Hu Y, Tong T, Peng X, Li M, Feng M, Cheng L, Ren B, Zhou X. 2018. ERG3 and ERG11 genes are critical for the pathogenesis of *Candida albicans* during the oral mucosal infection. Int J Oral Sci 10:9. https://doi.org/10.1038/s41368-018-0013-2.
60. Becker JM, Kauffman SJ, Hauser M, Huang L, Lin M, Sillaots S, Jiang B, Xu D, Roemer T. 2010. Pathway analysis of *Candida albicans* survival and virulence determinants in a murine infection model. Proc Natl Acad Sci U S A 107:22044–22049. https://doi.org/10.1073/pnas.1009845107.
61. Miyazaki T, Miyazaki Y, Izumikawa K, Kakeya H, Miyakoshi S, Bennett JE, Kohno S. 2006. Fluconazole treatment is effective against a *Candida albicans erg3/erg3* mutant *in vivo* despite *in vitro* resistance. Antimicrob Agents Chemother 50:580–586. https://doi.org/10.1128/AAC.50.2.580-586.2006.
62. Zhang L, Xu W. 2015. Histone deacetylase inhibitors for enhancing activity of antifungal agent: a patent evaluation of WO2014041424(A1). Expert Opin Ther Pat 25:237–240. https://doi.org/10.1517/13543776.2014.981256.
63. Mai A, Rotili D, Massa S, Brosch G, Simonetti G, Passariello C, Palamara AT. 2007. Discovery of uracil-based histone deacetylase inhibitors able to reduce acquired antifungal resistance and trailing growth in *Candida albicans*. Bioorg Med Chem Lett 17:1221–1225. https://doi.org/10.1016/j.bmcl.2006.12.028.
64. Hnisz D, Majer O, Frohner IE, Komnenovic V, Kuchler K. 2010. The Set3/Hos2 histone deacetylase complex attenuates cAMP/PKA signaling to regulate morphogenesis and virulence of *Candida albicans*. PLoS Pathog 6:e1000889. https://doi.org/10.1371/journal.ppat.1000889.
65. Pfaller MA, Messer SA, Georgopapadakou N, Martell LA, Besterman JM, Diekema DJ. 2009. Activity of MGCD290, a Hos2 histone deacetylase inhibitor, in combination with azole antifungals against opportunistic fungal pathogens. J Clin Microbiol 47:3797–3804. https://doi.org/10.1128/JCM.00618-09.
66. Pfaller MA, Rhomberg PR, Messer SA, Castanheira M. 2015. *In vitro* activity of a Hos2 deacetylase inhibitor, MGCD290, in combination with echinocandins against echinocandin-resistant *Candida* species. Diagn Microbiol Infect Dis 81:259–263. https://doi.org/10.1016/j.diagmicrobio.2014.11.008.
67. Smith WL, Edlind TD. 2002. Histone deacetylase inhibitors enhance *Candida albicans* sensitivity to azoles and related antifungals: correlation with reduction in CDR and ERG upregulation. Antimicrob Agents Chemother 46:3532–3539. https://doi.org/10.1128/AAC.46.11.3532-3539.2002.
68. Kim T, Buratowski S. 2009. Dimethylation of H3K4 by Set1 recruits the Set3 histone deacetylase complex to 5′ transcribed regions. Cell 137:259–272. https://doi.org/10.1016/j.cell.2009.02.045.
69. Pijnappel WW, Schaft D, Roguev A, Shevchenko A, Tekotte H, Wilm M, Rigaut G, Seraphin B, Aasland R, Stewart AF. 2001. The *S. cerevisiae* SET3 complex includes two histone deacetylases, Hos2 and Hst1, and is a meiotic-specific repressor of the sporulation gene program. Genes Dev 15:2991–3004. https://doi.org/10.1101/gad.207401.
70. Fingerman IM, Wu CL, Wilson BD, Briggs SD. 2005. Global loss of Set1-mediated H3 Lys4 trimethylation is associated with silencing defects in *Saccharomyces cerevisiae*. J Biol Chem 280:28761–28765. https://doi.org/10.1074/jbc.C500097200.
71. Harmeyer KM, South PF, Bishop B, Ogas J, Briggs SD. 2015. Immediate chromatin immunoprecipitation and on-bead quantitative PCR analysis: a versatile and rapid ChIP procedure. Nucleic Acids Res 43:e38. https://doi.org/10.1093/nar/gku1347.
72. Agarwal AK, Rogers PD, Baerson SR, Jacob MR, Barker KS, Cleary JD, Walker LA, Nagle DG, Clark AM. 2003. Genome-wide expression profiling of the response to polyene, pyrimidine, azole, and echinocandin antifungal agents in *Saccharomyces cerevisiae*. J Biol Chem 278:34998–35015. https://doi.org/10.1074/jbc.M306291200.
73. Dobin A, Davis CA, Schlesinger F, Drenkow J, Zaleski C, Jha S, Batut P, Chaisson M, Gingeras TR. 2013. STAR: ultrafast universal RNA-seq aligner. Bioinformatics 29:15–21. https://doi.org/10.1093/bioinformatics/bts635.
74. Anders S, Pyl PT, Huber W. 2015. HTSeq: a Python framework to work with high-throughput sequencing data. Bioinformatics 31:166–169. https://doi.org/10.1093/bioinformatics/btu638.

75. Givanna H Putri, Simon Anders, Paul Theodor Pyl, John E Pimanda, Fabio Zanini. 2022. Analysing high-throughput sequencing data in Python with HTSeq 2.0. Bioinformatics, btac166. https://doi.org/10.1093/bioinformatics/btac166.
76. Benjamini Y, Hochberg Y. 1995. Controlling the false discovery rate: a practical and powerful approach to multiple testing. J R Stat Soc Series B Statist Methodol 57:289–300. https://doi.org/10.1111/j.2517-6161.1995.tb02031.x.
77. Love MI, Huber W, Anders S. 2014. Moderated estimation of fold change and dispersion for RNA-seq data with DESeq2. Genome Biol 15:550. https://doi.org/10.1186/s13059-014-0550-8.
78. Zhang Y, Serratore ND, Briggs SD. 2017. N-ICE plasmids for generating N-terminal 3×FLAG-tagged genes that allow inducible, constitutive or endogenous expression in *Saccharomyces cerevisiae*. Yeast 34:223–235. https://doi.org/10.1002/yea.3226.
79. South PF, Fingerman IM, Mersman DP, Du HN, Briggs SD. 2010. A conserved interaction between the SDI domain of Bre2 and the Dpy-30 domain of Sdc1 is required for histone methylation and gene expression. J Biol Chem 285:595–607. https://doi.org/10.1074/jbc.M109.042697.
80. CLSI. 2008. Reference method for broth dilution antifungal susceptibility testing of yeasts; approved standard, 3rd ed. CLSI document M27-A3. Clinical and Laboratory Standards Institute, Wayne, PA.